**A Thesis for the Degree of Master of Engineering**

# Study on stability of curcumin-loaded filled hydrogel prepared using 4αGTase-treated rice starch

## 4αGTase 처리 쌀 전분을 이용한 커큐민 포접 필드하이드로겔의 안정성에 관한 연구

August 2020

Kang, Jihyun

Major of Biosystems Engineering

Department of Biosystems & Material Science and Engineering

Seoul National University

# Study on stability of curcumin-loaded filled hydrogel prepared using 4$\alpha$GTase-treated rice starch

## 4$\alpha$GTase 처리 쌀 전분을 이용한 커큐민 포접 필드하이드로젤의 안정성에 관한 연구

지도교수 김 용 노
이 논문을 공학석사 학위논문으로 제출함
2020년 7월

서울대학교 대학원
바이오시스템·소재학부 바이오시스템공학 전공
강 지 현

강지현의 공학석사 학위논문을 인준함
2020년 7월

| | | |
|---|---|---|
| 위 원 장 | 김 기 석 | (인) |
| 부 위 원 장 | 김 용 노 | (인) |
| 위 원 | 이 재 환 | (인) |

# Abstract

## Study on stability of curcumin-loaded filled hydrogel prepared using 4αGTase-treated rice starch

Curcumin is a primary natural polyphenol compound with antioxidant, anti-inflammatory, and anticancer properties. However, the application of curcumin is severely limited due to its low water solubility (11ng/mL) and bioavailability, and chemical instability to UV light and high temperature. In this study, filled hydrogels (1GS-FH, 24GS-FH, and 96GS-FH) by adding 4αGTase-treated rice starch (GS) prepared by treating rice starch with 4-α-glucanotransferase (4αGTase) for 1 h (1GS), 24 h (24GS), and 96 h (96GS) in aqueous phase of a curcumin-loaded emulsion. Emulsion (without adding any starch gel, EM) and native rice starch-based filled hydrogel (RS-FH) were prepared as control groups. The physicochemical properties of GS were analyzed first. GS showed decrease of molecular weight and a more gradual and flat chain length distributions in high-performance size exclusion chromatography (HPSEC) and high-performance anion exchange chromatography (HPAEC) analysis. In the texture profile analysis test, hardness of GS-FH decreased as enzyme treatment time increased. Moreover, the curcumin protection effects of FH system were

evaluated through UV stability (for 7 h), heat stability (for 24 h) and simulated gastrointestinal study in comparison with RS-FH and EM. The UV stabilities and curcumin retention after *in vitro* digestion of the FH samples were more improved than EM samples. RS-FH indicated 2.28-fold improved UV stability than EM due to the highest viscosity of RS. 1GS-FH, 24GS, and 96GS-FH increased curcumin retention by 2.31-, 2.45-, and 2.60-fold, respectively, and the microstructure of 96GS-FH using a confocal laser microscopy remained stable even after the stomach phase. For bioavailability measurements, the curcumin concentrations in all samples were extremely low, so accurate measurements could not be possible. Meanwhile, UV and heat stabilities of FH after freeze-drying (FH') was less effective than EM after freeze drying (EM'). However, FH' (especially GS-FH') still increased curcumin retention after *in vitro* digestion system. These effects may be attributed to the molecular structure of GS with smaller cyclic glucan and amylopectin cluster by modifying the molecular length and molecular weight of amylose and amylopectin. The encapsulation of lipids within the GS hydrogel particles served advantageously to protect and deliver the curcumin component, suggesting that GS-FH can be applied to gel-type food products that improve the chemical stability of curcumin.

**Keywords:** 4αGTase-treated rice starch; curcumin; filled hydrogel; stability; lipid digestibility; curcumin retention

***Student Number:*** 2018-23057

# CONTENTS

# LIST OF TABLES

# LIST OF FIGURES

# LIST OF IMAGES

# 1. Introduction

Curcumin [1,7-bis(4-hydroxy-3-methoxyphenyl)-1,6-heptadiene-3,5-dione] is a primary natural polyphenol compound found in the rhizome of *Curcuma longa* (turmeric) and in others Curcuma spp (Akram et al., 2010; Pulido-Moran et al., 2016; Wilken et al., 2011). It has a yellow-orange color, and has been widely used in food and many other industries due to its antioxidant, anti-inflammatory, and anticancer properties (AdityaandAdityaand et al., 2015; Pulido-Moran et al., 2016; ShenandJi, 2007). However, curcumin severely limits its application due to its low water solubility (11ng/ml) and bioavailability, and chemical instability to UV light and temperature (Ahmed K. et al., 2012; Nimiya et al., 2016).

Various systems, including emulsion, nanoemulsions, nanoparticles, and nanogels, have been studied to improve the stability and bioavailability of the curcumin (Zou et al., 2016). There have been many studies through various encapsulation methods using nature-derived materials, such as hydrophobically modified starch (HMS), β-cyclodextrin (CD) (Mangolim et al., 2014). In particular, encapsulating on the emulsion-based delivery systems, which is composed of emulsifier-surrounded lipid droplets dispersed within an aqueous phase, has been widely researched to allow curcumin to be released at a desirable site-of-action, or in accordance with a particular external stimulus and enhanced

the bioavailability (Joung et al., 2016; McClements D. et al., 2007; Pan et al., 2013; Zheng et al., 2017). However, the most widely used O/W emulsions are thermodynamically unstable and are often susceptible to decomposition over time or when exposed to certain environmental stress during production, storage, transport, and utilization (Ahmed K. et al., 2012). Moreover, they have limited a wide range of protective and delivery effects for certain types of bioactive compounds (Mun et al., 2015). Therefore, a new method of superimposing polysaccharides capable of increasing viscosity to the aqueous phase or forming gel networks on the O/W emulsions has been recently attempted to overcome these problems (Calero et al., 2013). This form is considered oil-in-water-in-water ($O/W_1/W_2$) emulsions, of which oil droplets are surrounded by hydrogel particles dispersed in an aqueous continuous phase containing a water-soluble emulsifier (McClements D. et al., 2007). Polysaccharide-based hydrogels, which are biomaterials such as biocompatibility and nontoxicity, are physicochemical cross-linked macromolecules that form a three-dimensional network capable of holding water without disintegration, and thus can serve as an ideal carrier for bioactive compounds (Jung et al., 2010; Lima-Tenório et al., 2015; Peppas et al., 2012). showed a more gradual and flat distributions

Rice starch, as a natural polysaccharide capable of forming a hydrogel, can be

used as a thickener, stabilizer, excipient, and fat mimetic in various foods (Do et al., 2012; Jung et al., 2010; Mitchell, 2009; Wani et al., 2012). However, since rice starch has irreversible high viscosity and thermal stability, many studies have tried to change the its physicochemical properties by enzyme treatment (Guraya et al., 2001; Khatoon et al., 2009; Mun et al., 2009). In particular, it is known that modification via 4-α-glucanotransferase (EC 2.4.1.25; 4αGTase), which can remodel parts of the amylose and amylopectin molecules by cleaving and reforming α-1,4- and α-1,6-glycosidic bond, delayed retrogradation of rice starch and improved thermal and pH reversible stability (Che et al., 2009; Lee K. Y. et al., 2006; Park H. R. et al., 2019; Takaha et al., 1996). In the previous study, a study using 4αGTase-treated rice starch (GS) as a wall material to improve the solubility, stability, and bioaccessibility of hydrophobic compounds was conducted (Park H. R. et al., 2019). In addition, a study was also attempted to use GS as a stabilizer to improve heating and shear stress by adding to the internal water phase of the W/O/W emulsion (Mun et al., 2011). However, no research has been conducted on filled hydrogels containing GS in the aqueous phase of O/W emulsions.

In this study, GS was used as a filled hydrogel material by the external water phase of $O/W_1/W_2$ emulsion. It was expected to effectively protect bioactive

compounds even in filled hydrogel systems due to unique molecular structural properties of GS. Therefore, the propose of this study was to establish the manufacturing conditions for GS-based filled hydrogel (GS-FH) with curcumin and investigate the effects of GS-FH on curcumin for storage, heat, UV stability, curcumin retention rate after *in vitro* digestion system and curcumin bioavailability. Emulsion (without adding any starch gel, EM) and native rice starch-based filled hydrogel (RS-FH) were prepared as a comparative system. Moreover, the gels produced by freeze-drying of FH and redistributed it again were compared to original FH by conducting the same above-mentioned experiment.

# 2. Objectives

The purposes of this studies are

1) to analyze the physicochemical properties of 4αGTase-treated rice starch

2) to optimize the conditions of production of curcumin-loaded filled hydrogel and microencapsulation powder

3) to estimate the chemical (heat, UV, and storage) stability of curcumin upon encapsulation

4) to analyze the bioaccessibility and bioavailability of curcumin in filled hydrogel and reconstituted gel of powder by *in vitro* model system

# 3. Background and Literature Review

## 3.1. Starch

### 3.1.1. Rice starch

Starch is plentiful, renewable storage polysaccharide produced by many plants and also the major source of carbohydrates in human diet (Le Corre et al., 2010; Raigond et al., 2015). It is used in various field of food and pharmaceutical industry. New application of starch includes biodegradable packaging materials, thermoplastic materials and low-calorie products (Biliaderis, 2009). Starch is a biopolymer and composed of two types of molecules: amylose (a linear polymer of α-D-glucose units) and amylopectin (a polymer of α-D-glucose units linked by α-1,4 and α-1,6 glycosidic linkages) (Singh et al., 2010; Zobel, 1988). Most starch contains 70-75% of amylopectin and 20-25% amylose contents. Amylose is actually helical and the interior of the helix includes hydrogen atoms, and therefore, its hydrophilic property allows to form a type of clatherate complex with other components (FennemaandPeterson, 1985). It has an average degree of polymerization (DP) value of 800 to 4920, average chain lengths (CL) of 250 to 670 (Wani et al., 2012). Especially, rice starch amyloses have 920 to 1110 DP values. Amylopectin molecules are highly branched and its structure is divided into A, B, and C chains (KossmannandLloyd, 2000). A chains (external chain)

are connected to B chain via their potential reducing end, and B chains are attached and carry one or more A chains (Wani et al., 2012). Lastly, C chains include the single reducing group of the amylopectin molecule and transfer other chains. Amylopectin has a DP of 4700 to 12800 and a CL of 17 to 24. In case of rice starch, it has a DP of 8200 to 12800, CL of 19 to 23 (Wani et al., 2012). Amylose and amylopectin have certainly different properties. Amylose is prone to retrogradation and form tough gels and strong films. Amylopectin, diffused in water, is more stable and form soft gels and weak films (PérezandBertoft, 2010).

Rice starch is identified as very small granules ranging between 2-8μm, which is much smaller than those of other tubers and roots (Dhital et al., 2015). Rice starch can be used as a substitute for gelatin used in dairy products. Rice starch can maintain a rigid gel structure. It also provides soft and creamy paste tastes for low-fat dairy products. However, native rice starches generally form cohesive, rubbery pastes when heated and undesirable gels when the pastes are cooled. Therefore, the food manufacturers commonly prefer starches which have better behavioral characteristic than those of native starches. The properties of starches can be developed by various modifications (Abbas et al., 2010).

### 3.1.2. 4αGTase-treated rice starch

*Thermocus aquaticus* α-1,4-glucanotransferase (4αGTase), which is a member of the α-amylase super-family (KurikiandImanaka, 1999). It is known that modification via 4-α-glucanotransferase (EC 2.4.1.25; 4αGTase), which can accelerates the hydrolysis of amylose molecules and remodel parts of the amylose and amylopectin molecules by cleaving and reforming α-1,4- and α-1,6-glycosidic bond, delayed retrogradation of rice starch and improved thermal and pH reversible stability (Che et al., 2009; Lee K. Y. et al., 2006; Park H. R. et al., 2019; Takaha et al., 1996). Furthermore, the enzymes catalyze intramolecular glucan transfer (cyclization reaction) within a single linear glucan molecule, producing a cycloamylose or cyclic glucan product, which is often referred to as a coupling reaction (Lee K. Y. et al., 2008; Strater et al., 2002; Takaha et al., 1996; Takaha et al., 1998). Modified starch with the 4αGTase has lower viscosity at proper concentrations after gelatinization or swelling and lower molecular weight and reassignment of amylopectin branch chains by hydrolytic and transglycosylation reaction.

## 3.2. Filled hydrogel

Hydrogel is a cross-linked polymeric network with the ability to absorb water, and three-dimensional hydrophilic structure (Ahmed E. M., 2015; Colombo, 1993). Hydrogels can be suggested with controllable responses with regard to shrink or expand with changes in external environment conditions (Ahmed E. M., 2015). Moreover, the cross-links between the polymer chains of hydrogels provide viscoelastic and sometimes pure elastic behavior, and gel structure (hardness) (Gulrez et al., 2011). With these characteristics, it has been used in a wide range of fields, including isolation of protein, cell encapsulation and drug release (Akhtar et al., 2016; Das, 2013).

Many researchers have developed hydrogels based on rice, potato, and soluble starches (Xiao, 2013; XiaoandYang, 2006). The formation of starch-based hydrogels is related to first starch gelatinization and then retrogradation owing to form a three-dimensional network (Biduski et al., 2018). The crystalline structure of starch is broken and connected between polymer chains during those processes. These starch-based hydrogels can be used in O/W emulsion systems as the form of filled hydrogel, which were added into the aqueous phase of emulsion. Oil-in-water (O/W) emulsions are often susceptible to decomposition over time or when exposed to certain environmental stresses during production,

storage, transport, and utilization (Ahmed, Li, McClements, & Xiao, 2012). Therefore, filled hydrogel system can be more stable than conventional O/W emulsion for bioactive protection and controlled bioactive release. This method is referred to as oil-in-water-in-water ($O/W_1/W_2$) emulsion, in which oil droplets are surrounded by hydrogel particles dispersed in an aqueous continuous phase containing a water-soluble emulsifier (McClements D. et al., 2007). Several studies have been conducted regarding this novel delivery system.

## 3.3. Curcumin

Curcumin [1,7-bis(4-hydroxy-3-methoxyphenyl)-1,6-heptadiene-3,5-dione] also called diferuloylmethane, is the main natural polyphenol found in the rhizome of *Curcuma longa* (turmeric) and in others Curcuma spp (Akram et al., 2010; Pulido-Moran et al., 2016; Wilken et al., 2011). It has a yellow-orange color so that which has attracted considerable concern in recent years (ShenandJi, 2007). In addition, it has been widely used in food and many other industries due to its antioxidant, anti-inflammatory, and anticancer properties (AdityaandAdityaand et al., 2015; Pulido-Moran et al., 2016). Curcumin is insoluble in water, but soluble in dimethyl sulfoxide, methanol, ethanol and

acetone (Ali et al., 2006). *Curcuma longa* contains others components called the curcuminoids group (Pulido-Moran et al., 2016). The naturally occurring ratios of curcuminoids in curcumin are about 3% bisdemethoxycurcumin, 17% demethoxycurcumin, 77% curcumin, and cyclocurcumin (Goel et al., 2008; Heger et al., 2014). Curcumin has a molecular weight of 368.37 $gmol^{-1}$ and a melting point of 183 ℃ (TapalandTiku, 2012). The methoxy groups on the phenyl rings in curcumin are important to have health effects (Pulido-Moran et al., 2016). Especially, the antioxidant activities of curcuminoids reduce the hemolysis and lipid peroxidation of erythrocytes (Perrone et al., 2015).

However, as mentioned above, curcumin has an extremely low water solubility (11ng/ml). In addition, effective properties of curcumin may not be realized even if it is ingested because of a low bioavailability of it (Ahmed K. et al., 2012). Moreover, curcumin is easily hydrolyzed in alkaline conditions and at higher pH (TonnesenandKarlsen, 1985; Wang Y.-J. et al., 1997). In acidic and neutral pH, the keto form of curcumin acts as a proton donor so that it is easily crystallized. Whereas, the alkaline condition above pH 8 changes the keto form to the enol form, and the curcumin functions as an electron donor which makes curcumin very unstable (Esatbeyoglu et al., 2012). Alkaline degradation of curcumin has been reported to offer ferulic acid and feruloylmethane, and latter may form vanillin and acetone by retro-aldol fission (RoughleyandWhiting, 1973). For this

reason, it is difficult to include curcumin in various products. Therefore, there are many methods have been studied to improve the solubility and bioavailability of the curcumin such as emulsion-based delivery system (Ahmed K. et al., 2012), polysaccharide-based hydrogel beads (Zhang Zipei et al., 2016), protein particles (Patel et al., 2010), and liposomes (Hasan et al., 2014). In this study, after curcumin was encapsulated into oil phase of emulsion and enzymatically modified starch was added the aqueous phase of emulsion to form filled hydrogel, curcumin stability and bioavailability was measured to effect of curcumin protection of filled hydrogel.

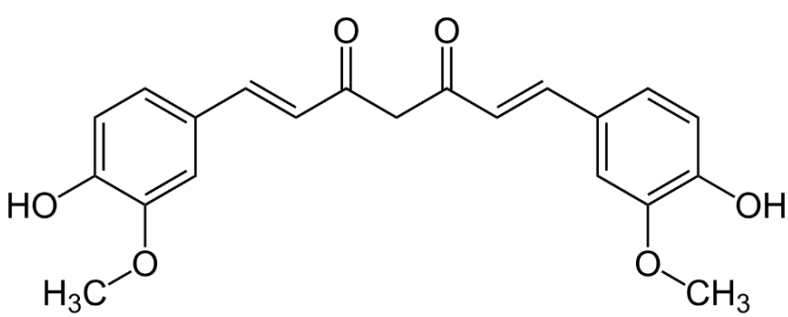


**Image 1. Molecular structure of curcumin**

# 4. Materials & methods

## 4.1. Physicochemical properties of enzymatic modified starch with 4αGTase treatment

### 4.1.1. Materials

The Ilpumbyeo rice cultivars were obtained from the Rural Development Administration of Korea. Luria-Bertani medium was purchased from Becton, Dickinson, and Company (Sparks, MD, USA). The 4-α-glucanotransferase (4αGTase) enzyme was produced by using a recombinant strain of *Escherichia coli* including thermostable 4αGTase gene isolated from *Thermus aquaticus* as described in the previous study (Park J.-H. et al., 2007). Hydrochloric acid (HCl) and sodium hydroxide (NaOH) were purchased from Duksan Pure Chemicals (South Korea). Other reagents were purchased from Daejung and Samchun Chemicals (South Korea). All chemicals and reagents used were of analytical grade.

### 4.1.2. Methods

#### 4.1.2.1. Isolation of rice starch

Starch used for this study was isolated from native rice (Ilpumbyeo, Korea) using a traditional alkaline method with a slight modification. The rice was washed and immersed in two volumes of distilled water for 2-3 h. The liquid was drained off and the grains were grounded in five volumes of 0.2 % v/v sodium hydroxide using a blender. The slurry was passed through 45, 100, and 270 mesh sieves in order, and the suspensions were left overnight. The supernatant was removed and the sediment was dissolved with NaOH solution. This process was repeated until the supernatant became clear and conducted a biuret reaction test to determine whether the protein remained. The separated starch was washed with distilled water, and neutralized using 1 N HCl. The sediments were collected and dried at room temperature for 5-6 days. The dried starch was grounded and then passed through 100 mesh sieve for using in study.

#### 4.1.2.2. Preparation of 4αGTase

##### 4.1.2.2.1. Transformation, Extraction and Purification of 4αGTase

To manufacture the 4-alpha-glucanotransferase (4αGTase), *Escherichia coli* MC 1061 was used as a host for DNA manipulation and transformation. The *E. coli* transformant including recombinant plasmid was cultured in LB medium containing ampicillin (100 μg/mL broth). *E. coli* cells were collected by centrifugation (3,699 g-force, 20 min, 4 ℃) and resuspended in lysis buffer (50mM Tris-HCl buffer (pH 7.5), 300 mM NaCl, 10 mM imidazole). The cell suspension was sonicated at an amplitude of 60%, and a duty cycle of 1 s (VCX-750, Sonics & Materials Inc., Newtown, CT. USA) and heated at 65 ℃ for 20 min to deactivate other enzymes. After the centrifuge was conducted once more (3,699 g-force, 20 min, 4 ℃), the supernatant was purified by using a nickel-nitrilotriacetic acid (Ni-NTA) column (Qiagen, Hilden, Germany) packed in a Poly-Prep Chromatography Column (0.8 x 4 cm; Bio-rad, USA). The final eluent was dialyzed against 50mM Tris-HCl buffer and stored at 4℃.

#### 4.1.2.2.2. Assay of 4αGTase activity

4-α-glucanotransferase activity was estimated by measuring the change in color in iodine-staining due to the conversion of amylose by the enzyme (LIEBL et al., 1992). The enzyme mixture was contained 250 μL of 0.2 % amylose, 50 μL of 1 % maltose, 600 μL of 50 mM Tris-HCl (pH 7.5) buffer, and 100 μL of enzyme solution. The mixture was heated at 75 ℃ for 10 min, and the reaction was discontinued by boiling for 10 min. Aliquots (0.1 mL) were mixed with 1 mL of Iodine solution (0.02 % (w/v) iodine and 0.2 % (w/v) potassium iodide), and the absorbance at 620 nm was measured with a UV/Vis spectrophotometer (UV-1650PC, Shimadzu Co., Japan). One unit of 4αGTase was defined as the amount of enzyme which degrades 0.5mg/mL of amylose per min under the assay condition.

#### 4.1.2.3. Preparation of 4αGTase-treated rice starch

4αGTase-treated rice starch (GS) was prepared according to the previous study (Park H. R. et al., 2019), with slight modification. Isolated rice starch (RS) was dispersed in distilled water (5% w/v) and boiled at 95 ℃ for 30 min with mechanical stirring. After cooling to 75 ℃, 4αGTase (20 U/g, dry basis) was added to starch pastes and incubated at 75 ℃ for 1 h (1GS), 24h (24GS) and 96 h (96GS) with constant stirring. The enzyme reaction was boiled at 95 ℃ for 10 min, and then a 5-fold volume of 95% ethanol was mixed with dispersions to precipitate the starch. The mixtures were centrifuged (7,167 ×g, 15 min) and the sediments were dried in a dry oven at 40 ℃. The modified starch was finely ground and passed through a 100-mesh sieve prior to use.

#### 4.1.2.4. Physicochemical properties of 4αGTase-treated rice starch

##### 4.1.2.4.1. Molecular weight distribution (HPSEC)

The molecular weight distributions of starch samples were determined by the high-performance size exclusion chromatography (HPSEC). Starch samples (RS, 1GS, 24GS and 96GS) were dispersed (1% w/v) in 90% DMSO solution and boiled for 1 h with stirring. Then, the hot solution was continuously stirred for 24 h at room temperature for accomplishing a complete dissolution of starch. To precipitate the starch, a 5-fold volume of 95% (v/v) ethanol was added to the starch dispersions and centrifuged at 12,741 ×g for 15 min. The sediments were washed with a 2-fold volume of acetone and centrifuged under the same condition. The pellets were dried in a dry oven for 2-3 days. The pretreated samples were redissolved in boiling water (0.5% w/v) with vortexing at 5 min intervals. The hot samples were filtered through a 5.0 μm disposable membrane filter and then injected into a HPSEC system consisted of a refractive index detector (ProStar 355 RI Detector; Varian, Australia), and two running columns (PH-Pak 804 and OH-806 HQ; Shodex). The flow rate of the mobile phase (HPLC grade water, J.T.Baker, Deventer, Netherlands) was 0.4 mL/min and the columns were run at 50 °C. The molecular weight distribution of starch samples was determined using Pullulans standards (Shodex Standards, Japan).

#### 4.1.2.4.2. Distribution of branched chain length (HPAEC)

The pretreatment procedure of starch samples for high-performance anion exchange chromatography (HPAEC) analysis was exactly the same as for HPSEC analysis. The pretreated starch samples (0.25%, w/w) were resuspended with 50mM sodium acetate buffer (pH 4.5) and boiled for 15 min with vortexing intermittently. Then, 1 U/mg of isoamylase (Megazyme, Wicklow, Ireland) was added to the solution and incubated at 40 ℃ for 2 h in order to debranch the starch side chains. To finish the enzyme reaction, the sample solutions were boiled for 10 min and filtered using a 0.45 μm membrane filter and analyzed using the HPAEC system with a CarboPac TM PA1 column (4 × 250 mm, Dionex, USA). The filtered sample solutions were separated using gradient eluents with 0.150 M sodium hydroxide and 0.15 M sodium hydroxide in 0.6 M sodium acetate solution at a flow rate of 1.0 mL/min. All of the measurements were operated at a flow rate of 1.0 mL/min, and the gradient condition is shown in Table 1.

**Table 1. HPAEC solvent gradient condition**

| Time (Che et al.) | 0 | 10 | 16 | 27 | 44 | 63 | 70 | 70.01 | 75.01 | 80.01 |
|---|---|---|---|---|---|---|---|---|---|---|
| **Buffer A (%)** | 90 | 70 | 60 | 50 | 40 | 35 | 34 | 0 | 100 | 90 |
| **Buffer B (%)** | 10 | 30 | 40 | 50 | 60 | 65 | 66 | 100 | 0 | 10 |

Buffer A: 0.150 M sodium hydroxide

Buffer B: 0.150 M sodium hydroxide in 0.6 M sodium acetate

#### 4.1.2.4.3. Rheological properties

The rheological properties of the starch samples were analyzed with a rheometer (AR1500ex; TA Instruments Ltd., New Castle, DE, USA). A parallel plate geometry with a diameter of 0° 20 mm was used. After boiling starch samples (10 % w/v) for 1 h, the hot samples were transferred to the bottom plate and pressed by upper parallel with a 1 mm gap between. The excess suspension was discarded and a thin layer of silicon oil was placed around the edge of plate to minimize loss of moisture during the measurements. During the gelation kinetics measurements, three oscillation tests were done. The three steps were conducted consecutively:

(1) Time sweep test - Time: 15 min (RS); 24 h (GS), Frequency: 1 Hz, fixed strain: 0.5 %

(2) Frequency sweep - Frequency: 0.1 to 1 Hz, fixed strain: 0.5 %, Temperature: 25 ℃

(3) Temperature ramp - Temperature: 4 to 85 ℃, heating rate: 5 ℃/min, Frequency: 1 Hz, fixed strain: 0.05 %

#### 4.1.2.4.4. Viscosity analysis

Viscosity was evaluated according to Chen et al. (2018) with some modifications. Steady-state flow was measured using an rheometer (AR1500ex; TA Instruments Ltd., New Castle, DE, USA) with a 0° 20 mm parallel plate geometry. The starch samples were mixed with distilled water (10% w/v) and heated at 95 ℃ for 1 h. Then the hot suspensions were loaded on the bottom plate and pressed by the top plate with a 1 mm gap between. The excess suspension was trimmed away, and the edge of the plate was covered with a silicon oil to prevent evaporation during measurements. The viscosity test was equilibrated at 25 ℃ for 1 min before the measurements and measured with the shear rate range of 0.1-100 $s^{-1}$ and a sample period of 10 sec. The consistency index and flow behavior index of each sample was calculated on the basis of the following power law equation:

$$\tau = K\gamma^{n}$$

where τ is the shear stress (Pa), $K$ is the consistency index ($Pa \cdot s^{n}$), γ is the shear rate ($s^{-1}$), and $n$ is the flow behavior index (dimensionless).

#### 4.1.2.4.5. Granular morphology

The granular morphology of RS, 1GS, 24GS, and 96GS were observed using field-emission scanning electron microscopy (SEM) (SUPRA 55VP, Carl Zeiss, Germany). The sieved samples were placed on double-sided carbon tape and coated with a 20-nm-thick platinum film under a vacuum at 20 mA for 180 s. The samples were observed by SEM at 2.00 kV. Micrographs of each sample were taken at × 30K (RS), × 150K (1GS, 24GS, and 96GS) magnification.

#### 4.1.2.4.6. Starch crystallinity

The X-ray diffraction pattern and degree of crystallinity of the samples were observed using an X-ray diffractometer (D8 Advance, Bruker, Germany, Detector: LYNXEYE XE). The X-ray diffractograms were obtained under conditions of 40 kV and 40 mA with Cu Kα1 radiation of 1.5418 A. The samples were scanned on aluminum trays (sample layer, 15 × 20 × 1.5mm) at diffraction angles (2θ) from 5-40 ° (step size 0.02 °, time per step 0.5 s).

### 4.1.2.4.7. Iodine absorption capacity

Iodine absorption capacity of starch samples was conducted using an amylose-iodine absorption method with slight modification (KnustonandTao, 1999). The samples were dispersed in 90% DMSO solution (0.5% w/v) with mechanical stirring. The solutions were diluted in 50-fold distilled water, and 4 ml of the diluted solution was mixed with 800 μl of the iodine solution (0.0025 M $I_2$ and 0.0065 M KI). The changed color was read after 5 min at wave scanning from 400 to 800 nm using an UV/Vis spectrophotometer (UV-1650PC, Shimadzu Co., Japan).

### 4.1.2.5. Statistical analysis

In this study, all the experiments were performed duplicate or triplicate and presented as the mean and standard deviation (mean ± SD). All data were analyzed by the one-way ANOVA test followed by a Duncan's multiple range test for mean using SPSS for windows (ver. 25.0; IBM Corp., Armonk, N.Y., USA). A value of $p < 0.05$ was considered statistically significant between the data.

## 4.2. Encapsulation of the curcumin in filled hydrogel & microencapsulation powder

### 4.2.1. Materials

4αGTase-treated rice starch (1GS, 24GS, and 96GS) was prepared in the first part of the study. Curcumin (curcuminoid content ≥ 94%), mucin (from porcine stomach), bile extracts (from porcine), pepsin (from porcine gastric mucosa), and pancreatin (from porcine pancreas) were purchased from Sigma-Aldrich (St. Louis, MO, USA). Soybean oil (Ottogi Corp., Pyeongtaek, Korea) was obtained from a local market. Whey protein isolate (WPI, product code: 9500) was provided by Protient, Inc (St. Paul, MN, USA). 3-(4,5-dimethyl thiazol-2-yl)-2,5-diphenyltetrazolium bromide (MTT) was provided by Duchefa Biochemie (Haarlem, Netherlands). Dulbecco's modified eagle media (DMEM) and fetal bovine serum (FBS) were purchased from Hyclone (Logan, UT, USA). All chemicals and reagents were used were of analytical grade.

### 4.2.2. Methods

#### 4.2.2.1. Fabrication of curcumin-loaded filled hydrogel

##### 4.2.2.1.1. Preparation of curcumin-loaded O/W emulsion

Curcumin-loaded O/W emulsion (EM) was manufactured by the procedure described in Ahmed K. et al. (2012) with slight modification (Fig. 1A). The oil phase was produced by adding curcumin (0.3%, w/w) in soybean oil and heating at 60 ℃ for 10 min with stirring magnetically. Then, the heated oils were sonicated (Ultrasonic Cleaner-Powersonic 410, Hwashin, Seoul, Korea) for 30 min and centrifuged (1,170 ×g, 10 min) to separate the supernatant only. WPI (3%, w/w) was dissolved in 5mM phosphate buffer (pH 7.0) for 1 h with stirring gently. A coarse emulsion (30 wt% oil) was prepared by homogenizing curcumin-containing soybean oils and WPI solutions using a high-speed blender (ULTRA-TURRAX model T25 digital, IKA, Germany) for 2 min and then passing the stock emulsion through a micro-fluidizer (Picomax MN 250A, Micronox, Seongnam, Korea) three times at 10,000 psi. In the experiment, emulsion with 4 wt % oil was used by diluting stock emulsions with 5 mM phosphate buffer (pH 7.0).

#### 4.2.2.1.2. Preparation of filled hydrogel with starch

Filled hydrogel was prepared through the process as shown in Fig. 1A. The starch sample was dispersed in distilled water (10%, w/w) and boiled at 90 ℃ for 15 min to complete dissolution. Stock emulsion (30 wt% oil) was then blended smoothly with the hot starch solution using a glass rod to adjust the oil concentration of the filled hydrogel to 4% (w/w). The heated mixtures were transferred to flat petri dishes, left at room temperature until cooled, and then stored at 4 ℃ overnight to form a gel. Native rice starch-based filled hydrogels were compared with emulsion systems. As shown in Fig. 1, samples were labelled with curcumin-loaded emulsion (EM), curcumin-loaded native rice starch based filled hydrogel (RS-FH), and curcumin-loaded 4αGTase-treated rice starch based filled hydrogel (1GS-FH, 24GS-FH and 96GS-FH).

**(A)**

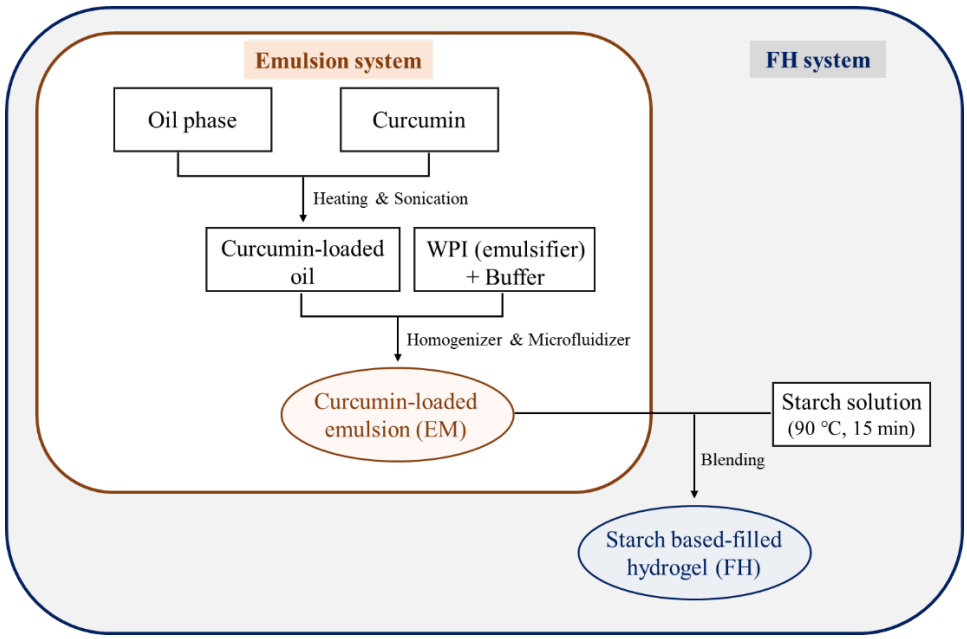


**(B)**

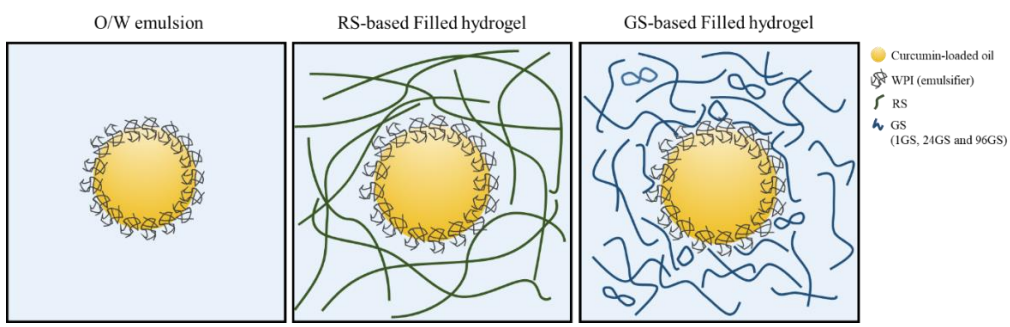


**Fig. 1. (A) Flow chart of manufacturing process (B) schematic representation of curcumin encapsulation system prepared in this study.**

#### 4.2.2.2. Characteristics of curcumin-loaded filled hydrogel

##### 4.2.2.2.1. Rheological properties of filled hydrogel

Rheological properties of filled hydrogel were evaluated in the same way as above (section 4.1.2.4.3. and 4.1.2.4.4.). The dynamic viscoelastic properties of filled hydrogel and steady shear viscosity of the starch and filled hydrogel samples were conducted using an AR1500ex rotational rheometer (TA Instruments Ltd., New Castle, DE, USA) with a 0° 20 mm parallel plate geometry. The starch samples were prepared by mixing with distilled water (10 %, w/w) and heating at 95 ℃ for 1 h and the filled hydrogel samples were also prepared in the same way as the above of making filled hydrogel (section 4.2.2.1.2.). Then, the hot samples were transferred to the bottom plate and pressed by upper parallel with a 1 mm gap between. The excess suspension was trimmed away, and the edge of the plate was covered with a silicon oil to prevent evaporation during measurements. The dynamic frequency sweep test was performed at 25 ℃ at a constant strain (0.5%), over a frequency range between 0.1 and 10 frequency (Hz). The steady shear viscosity test was equilibrated at 25 ℃ for 1 min before the measurements and measured with the shear rate range of 0.1-100 $s^{-1}$ and a sample period of 10 sec. The consistency index and flow behavior index of each sample was calculated on the basis of the following power law equation:

$$\tau = K\gamma^n$$

where τ is the shear stress (Pa), $K$ is the consistency index (Pa·s$^n$), γ is the shear rate (s$^{-1}$), and $n$ is the flow behavior index (dimensionless).

#### 4.2.2.2.2. Texture profile analysis (TPA)

Cylindrical gel samples (35 mm diameter, 10 mm height) were placed on the platform and a TPA test was carried out with a TA-HDi texture analyzer (Stable Micro Systems Ltd, Godalming, UK) using a P50 aluminum probe. The samples were compressed twice at a speed of 1 mm/s with a 40% strain. Samples in triplicates were tested for textural parameters to measure how the filled hydrogel behaved when compressed to a large extent of deformation.

#### 4.2.2.3. Fabrication of curcumin-loaded microencapsulation powder and reconstitution

After manufacturing the filled hydrogel, the samples were put into the falcon tube wrapped by foil and drilled holes, and stored in deep freezer for a day. When the samples were frozen, freeze-dried for 4 days until complete dehydration (FD8508, Ilshin BioBase, Korea). The final products were grounded and stored at – 20 ℃ for further analysis. Samples were labelled with EM powder (Perrone et al.), RS-FH powder (RS-FHP), and GS-FH powder (1GS-FHP, 24GS-FHP and 96GS-FHP).

For stability analysis, digestibility test, bioaccessibility, and bioavailability evaluation, the powders were reconstituted by dissolving in distilled water (amounts of dehydration) and heating at 60 ℃ for 10 min for complete dissolution. The heated mixtures were placed on flat petri dishes, left at room temperature until cooled, and then stored at 4 ℃ overnight to form a reconstituted gel. Samples were labelled with reconstituted EMP (EM'), reconstituted RS-FHP (RS-FH'), and reconstituted GS-FHP (1GS-FH', 24GS-FH' and 96GS-FH').

#### 4.2.2.4. Characteristics of microencapsulation powder

##### 4.2.2.4.1. Morphology of microencapsulation powder

Morphology of the curcumin-microencapsulation powder was observed by field-emission scanning electron microscopy (SEM) (SUPRA 55VP, Carl Zeiss, Germany). Pure curcumin (Cur), starch samples (RS, 1GS, 24GS, and 96GS), the curcumin-microencapsulation powder (RS-FHP, 1GS-FHP, 24GS-FHP, 96GS-FHP) were imaged. The sieved samples were placed on a carbon tape and coated by Platinum film under vacuum condition at 20 mA for 180 sec. The coating thickness of the Platinum was 20 nm. The samples were observed by SEM at 2.00 kV, and micrographs of each sample were taken at × 2K (Cur), × 5K (RS, 1GS, 24GS, 96GS; EMP, RS-FHP, 1GS-FHP, 24GS-FHP, 96GS-FHP) magnification.

##### 4.2.2.4.2. Fourier Transform Infrared Spectroscopy (FT-IR)

To perform FT-IR measurements using a Fourier transform infrared spectrometer (TENSOR27, Bruker, Germany), dry samples (curcumin, starch samples, EMP, physical mixtures (EMP and each starch), FHP) were equilibrated at laboratory humidity and clamped directly onto the crystal. 32 spectra were acquired and co-added for each sample at a resolution of 4 $cm^{-1}$. The spectral range was 400-4000 $cm^{-1}$ per samples.

#### 4.2.2.5. Curcumin stability analysis of filled hydrogel and micro-encapsulation powder

##### 4.2.2.5.1. Heat stability

Heat stability was analyzed according to Li M. et al. (2014) with slight modification. The small amounts of samples (EM, EM', 1GS-FH, 1GS-FH', 24GS-FH, 24GS-FH', 96GS-FH, 96GS-FH') were heated in a water bath at 95°C for 0, 10 min, 30 min, 2, 6, 8, 24 h. The samples were cool down to room temperature promptly. Then, gel-type samples were mixed with a 12-fold of acetone and centrifuged at 1,210 ×g for 15 min. While, the emulsion samples (EM and EM' were mixed with isooctane/2-propanol (3:2, v:v, and centrifuged at 1,210 ×g for 3 min. The supernatant (gel-type samples) and bottom layer (EM and EM') were filtered using a 0.45 μm PVDF membrane filter respectively and measured spectrophotometrically at 430 nm. The remaining concentration of curcumin was calculated based on the curcumin standard curve suitable each solvent. All tests were performed in triplicate.

#### 4.2.2.5.2. UV stability

UV stabilities of curcumin loaded in starch-based filled hydrogels and reconstituted gels were conducted under UVB irradiation chamber. The forms of curcumin-loaded emulsion and reconstituted emulsion were also examined as a control. The small amounts of samples were placed on a rotating plate and then exposed to UV radiation (TUV 8W G8T5, Philips, Poland) for a set time (0, 1, 3, 5, and 7 hours). Afterward, gel-type samples were mixed with a 12-fold of acetone and centrifuged at 1,210 ×g for 15 min. Whereas, the emulsion samples (EM and EMP-R) were mixed with isooctane/2-propanol (3:2, v:v), and centrifuged at 1,210 ×g for 3 min. The supernatant (gel-type samples) and bottom layer (EM and EM') were filtered through a 0.45 μm PVDF membrane filter respectively and analyzed spectrophotometrically at 430 nm. The curcumin content was calculated based on the curcumin standard curve suitable each solvent. All tests were performed in triplicate.

#### 4.2.2.6. Curcumin retention rate & bioavailability analysis of curcumin in filled hydrogel and microencapsulation powder

##### 4.2.2.6.1. In vitro digestibility test

Samples were passed through a gastrointestinal tract (GIT) model that consists of oral, gastric, and intestinal phases to simulate the biological fate of the encapsulated curcumin after digestion. This model was consulted the method has been described in detail in previous studies (Mun et al., 2015; Zhang R. et al., 2015).

**Oral phase**: Simulated saliva fluid (SSF) prepared in accordance with a previous study (Sarkar et al., 2009), was mixed with mucin in advance. Then, α-amylase was added to this mucin solution and warmed up to 37 ℃ before starting the experiment. The mixture was adjusted to pH 6.8 by adding 1M NaOH solution. The samples (curcumin, emulsion, and filled hydrogel) were blended with the mucin solution at a 1:1 ratio and incubated at 37 ℃ for 10 min with constant stirring.

**Gastric phase**: Simulated gastric fluid (SGF) was prepared using a method described by (Sarkar et al., 2009). Pepsin solution was manufactured with mixing SGF and pepsin, and added to the sample from the oral phase at a 1:1 ratio. The pH of the mixture was adjusted to 2.5 using 1M NaOH and incubated at 37 ℃

for 2 h with continuous stirring.

**Small intestinal phase**: To simulate the circumstances in the small intestinal phase of the GIT, a pH-stat automatic titration unit (Metrohm USA Inc, River-view, FL) was used in this study (Mun et al., 2015). After gastric digestion phase, the samples were adjusted to pH 7 and bile extract and salt solution were then added. The mixture was adjusted once again to pH 7. Afterward, pancreatin suspension was added and the sample solution was incubated at 37 ℃ for 2 h with stirring constantly. The pH of the mixture was monitored, recording the volume of 0.25 M NaOH required to neutralize the mixture during two hours. The percentage of free fatty acid (FFA) released was calculated following equation, which presuming that 2 FFAs and a monoacylglycerol are released per triacylglycerol molecule by the lipase reaction:

$$\% \text{ FFA} = 100 \times \frac{V_{NaOH} \times m_{NaOH} \times M_{lipid}}{w_{lipid} \times 2}$$

where $V_{\text{NaOH}}$ is the volume of titrant in liters, $m_{\text{NaOH}}$ is the molarity of sodium hydroxide, $M_{\text{lipid}}$ is the molecular weight of soybean oil (920 g/mol), and $w_{\text{lipid}}$ is the weight of oil in the digestion system in grams. Blanks (samples without oil) were carried out, and the volume of titrant used for these sample was subtracted from the corresponding samples containing oil.

#### 4.2.2.6.2. Confocal laser scanning microscopy (CLSM)

Structural changes of lipid droplets during the digestive process were obtained by using confocal laser scanning microscopy (Leica TCS SP8 X, Leica Micro-systems, Wetzlar, Germany). The samples acquired from the different stages (initial, mouth, stomach, and intestine) of the GIT were dyed with Nile red dissolved at 0.01% (w/v) in ethanol. The fluorescently labelled samples were placed on glass slide. Then, the samples were examined using a 63 × oil immersion objective lens. Nile red was excited at a wavelength of 488nm. All captured images were processed using the Leica software program (Leica application suite X (LAS X), Leica Micro-systems, Wetzlar, Germany).

#### 4.2.2.6.3. Curcumin retention rate

Curcumin retention was quantified as the remaining amount of curcumin in digesta after *in vitro* digestion system. The raw digesta, collected after the small intestinal stage, were then mixed with chloroform at 1:1 ratio and centrifuged at 315 ×g for 10 min using a centrifuge (Supra 22 K, Hanil Science Inc., Incheon, Korea) to extract curcumin in the sample mixture. The extracted curcumin was collected from the bottom layer, and examined on a UV-vis spectrophotometer (UV-1650 PC, Shimadzu, Kyoto, Japan) at 430 nm with pure chloroform as a blank. The initial samples before digestive process were determined as a control. The curcumin retention was calculated in the following equation:

$$\text{Curcumin retention (\%)} = \frac{\text{Curcumin concentration in raw digesta}}{\text{Initial curcumin concentration}} \times 100$$

#### 4.2.2.6.4. Curcumin bioavailability analysis

##### 4.2.2.6.4.1. Caco-2 cell culture

The Caco-2 cell line (human epithelial colorectal adenocarcinoma) was obtained from Korean Cell Line Bank (KCLB #30037.1; Seoul, Korea). The cells were cultured in Dulbecco's modified eagle media (DMEM) supplemented with 10% fetal bovine serum, 2% L-glutamine, 1% penicillin (10,000 Units/mL) and streptomycin (10,000 µg/mL). The cells were incubated at 37 ℃ in a $CO_2$ incubator (BF-40 Cl; Biofree, Seoul, Korea). The incubator had an atmosphere of 95% air and 5% $CO_2$ (Bhushani et al., 2016). Cells were harvested at 70-80% confluence by trypsinisation with 0.05% trypsin-EDTA and resuspended in medium. Consequently, the cells were seeded at a density of $4.5 \times 10^5$ cells per well onto Transwell® polycarbonate inserts (4.52 $cm^2$ growth area; SPL Life Science Co., Seoul, Korea) placed in 6 well plate, which was coated with Matrigel™ basement membrane matrix (Corning, New York, NY, USA) beforehand. Caco-2 cells were grown for 21 days to form a confluent monolayer and the growing medium was replaced once every two days.

After 21 days, the TEER value (expressed as Ω (TEER (Ω) – $TEER_{background}$ (Ω)) × $cm^2$ (area)) was measured using an Evohm2 epithelial voltohmmeter (World Precision Instruments, Sarasota, FL) to check the integrity of Caco-2

monolayers. TEER values were more than 300 Ω × $cm^2$ prior to the experiment (Liu D. et al., 2018; Wang L.-L. et al., 2018). The Caco-2 cell experiment was carried out to a minimum with samples expected to show a marked difference in results (Cur, RS-FH, RS-FH', 96GS-FH, 96GS-FH').

#### 4.2.2.6.4.2. MTT cytotoxicity assay

Caco-2 cell cytotoxicity was determined according to a previous study with slight modification (Jin et al., 2020). The cells were harvested and seeded in 96-well plates at a density of 1 × $10^4$ cells per well. The raw digesta after *in vitro* digestion system was diluted in half and prepared up to 256 times in 8 different concentrations. The diluted samples were loaded onto 96-well plates and incubated for 2 h. The solution without sample was used as a control. Then, 10 μL of MTT solution was added to each well and incubated for 4 h (37 ℃, 5% $CO_2$). Afterwards, 100 μL of solubilization solution (0.01 M HCl + 10% SDS) was added and incubated overnight. The absorbance was analyzed at 570 nm using a microplate reader (SpectraMax® M3, Molecular Devices). The percent cell viability was measured according to equation. The experiment was conducted at concentrations with a cell viability of more than 80%.

$$Cell\ viability\ (\%) = \frac{Absorbance\ of\ the\ sample}{Absorbance\ of\ the\ control} \times 100$$

### 4.2.2.6.4.3. Curcumin bioavailability

Curcumin bioavailability was performed according to the procedure described by previous studies (AdityaandYangand et al., 2015; Bhushani et al., 2016). The samples were diluted to the concentration obtained by the cytotoxicity assay. Media was removed from transwells and 1.5 mL of fresh media was added to basolateral side of transwell system. Then, 1.5 mL of diluted sample was loaded onto apical side. After incubation for 2 h, insert was removed from the plate and the collected solution from the basolateral side was transferred to the falcon tube. The solutions were mixed with a 2-fold of acetonitrile and centrifuged (10,000 ×g, 3 min) at 4 ℃. The supernatants were concentrated using a nitrogen evaporator (MG-3100, Eyela, Tokyo, Japan). Finally, the pellets were dissolved in 100 μL mobile solvent of HPLC, and filtered through a 0.25 μm disposable membrane filter. Curcumin concentrations were quantified by HPLC. Bioavailability was calculated according to equation.

$$Bioavailability\ (\%) = \frac{curcumin\ (basolateral)}{curcumin\ (apical)} \times 100$$

where curcumin (apical) is the amount of curcumin added to the apical side of transwell plate, and curcumin (basolateral) is the amount of curcumin permeated from the apical side.

#### 4.2.2.6.4.4. Determination of curcumin content

HPLC determination of curcumin was performed following a method of previous study with modification (YuandHuang, 2011). Curcumin content was quantified by high-performance liquid chromatography (HPLC; Agilent 1100 series, Agilent Technologies, Santa Clara, CA, USA) equipped with a variable wavelength detector, on a Nova-Pak C18 3.9 × 150 mm column at 420 nm wavelength. Mobile phase solvents were 60% water containing 1% citric acid and 40% (v/v) tetrahydrofuran, adjusted to pH 3.0 with concentrated KOH solution. Flow rate and injection volume were 1 mL/min and 20 μL, respectively.

### 4.2.2.7. Statistical analysis

All the experiments carried out in this study were performed duplicate or triplicate and presented as the mean and standard deviation (mean ± SD). All data were analyzed by the one-way ANOVA test followed by a Duncan's multiple range test for mean using SPSS for windows (ver. 25.0, IBM Corp., Armonk, N.Y., USA). A value of $p < 0.05$ was considered statistically significant between the data.

# 5. Results and discussion

## 5.1. Physicochemical properties of enzymatic modified starch with 4αGTase treatment

### 5.1.1. Molecular weight distribution (HPSEC)

After the rice starch reacted with enzyme for 1 h, 24 h and 96 h, the molecular weight distribution of the 4αGTase-treated rice starch (1GS, 24GS and 96GS) was determined by high pressure size exclusion chromatography (HPSEC), and the result was compared with that of native rice starch in Fig. 2. The molecular weight distribution of RS indicated a bimodal shape: fraction I (retention time, 18-30 min) of high $M_w$ in accord with amylopectin, and fraction II (retention time, 32-45 min) of lower $M_w$ corresponded to amylose (Do et al., 2012; Lii et al., 1996). Meanwhile, the fraction I of 4αGTase-treated rice starch (GS) gradually decreased and fraction II region of GS increased as the enzyme treatment time increased, which is consistent with Do et al. (2012). After 24 h and 96 h of enzyme treatment (24GS and 96GS), the highest peak molecular weight of the fraction II was shifted from $2.12 \times 10^5$ g/mol to $2.28 \times 10^4$ g/mol and the fraction I region was largely disappeared (Guraya et al.). In addition, the relative peak intensity of the fraction II of 96GS was 3.56 times higher than that of 1GS. This result was attributed to the production of amylopectin cluster with reduced size as a result of rearrangement of the amylopectin inner and outer branch chains of

rice starch via disproportionation action of the 4αGTase (Kim Y.-L. et al., 2017). In addition, previous research reported that the amylose content of rice starch was significantly reduced by 4αGTase. Therefore, amylopectin as well as amylose molecules could also contribute to the decrease in relative molecular weight by hydrolysis and/or cycloamylose production through an intramolecular glucan transfer action by enzyme (Cho et al., 2009; Park J.-H. et al., 2007).

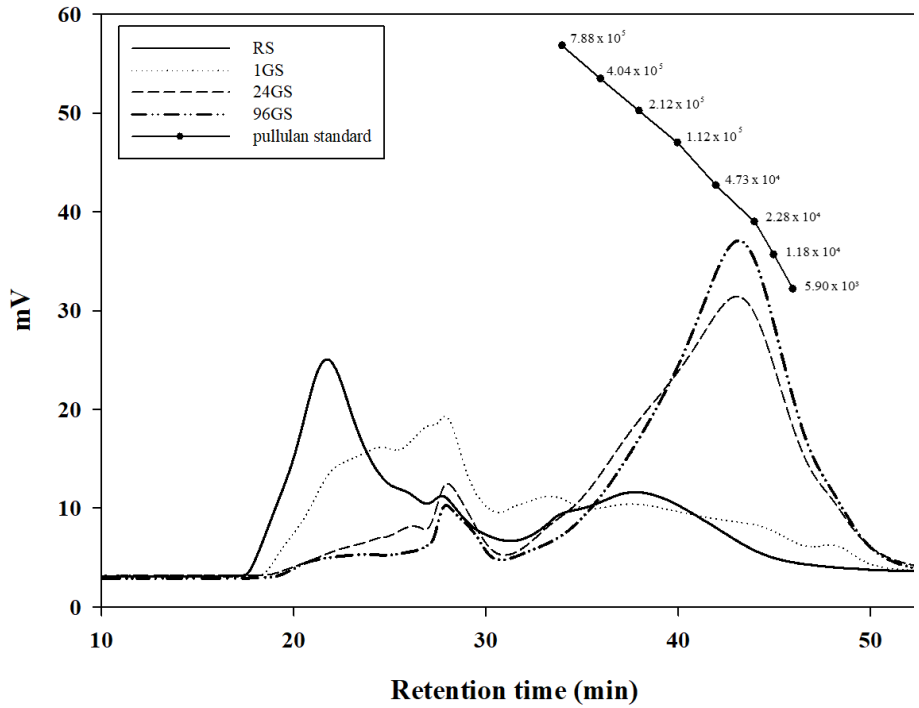


**Fig. 2. Molecular weight distributions of native rice starch (RS) and 4αGTase-treated rice starch (1GS, 24GS, and 96GS) with pullulan standard**

### 5.1.2. Distribution of branched chain length (HPAEC)

The branched chain length distributions of RS, 1GS, 24GS, and 96GS measured by high-performance anion exchange chromatography (HPAEC) are shown in Fig. 3 and Table 2. The chain length distributions of RS before 4αGTase treatment represented a sharp horn-like shape with DP 12 at the apex, while those of GS showed a more gradual and flat distributions from DP 3 to DP 62. The most conspicuous alteration by treating enzyme was that the relative proportions of A chains, $B_2$ chains, and $B_3$ chains increased, while those of $B_1$ chains decreased, which is consistent with previous studies (Kim YangandTrinh Khanh Sonand et al., 2012; Park H. R. et al., 2019). 4αGTase rearranges parts of the amylose and amylopectin molecules by cleaving and reforming α-1,4- and α-1,6-glycoside bonds (Kaper et al., 2004; Kim YangandTrinh Khanh Sonand et al., 2012). This enzyme also sensitively catalyzes the external branch chains (A and $B_1$ chains) of amylopectin to redistribute the chain length more evenly and catalyzes the internal chains ($B_2$ and $B_3$ chains) of amylopectin to involve in the interconnection of short chain clusters (Do et al., 2012). Thus, the increase in the long-branched chains ($B_2$ and $B_3$ chains) may be due to the cleaved amylose and short-branched chains of amylopectin ($B_1$ chains) being shuffled to other non-reducing ends of amylopectin chains via catalysis of intermolecular

transglycosylation by enzyme (van der MaarelandLeemhuis, 2013). In addition, a slight increase in proportion of A chains (DP ≤ 12) after enzyme treatment were probably due to the partial hydrolysis and/or intramolecular rearrangement of branched chains of amylopectin (Kim YangandKim Young-Limand et al., 2012).

Meanwhile, the relative portion of the long-branched chains ($B_2$ and $B_3$ chains) of 96GS was slightly reduced (1GS, 31.15%; 24GS, 30.32%; 96GS, 29.66%) and that of the short-branched chains ($A_1$ chains) was increased (1GS, 31.19%; 24GS, 33.59%; 96GS, 34.00%) compared to 1GS and 24GS. This could be due to the cleavage of the internal chains and/or the formation of cyclic glucans by intramolecular transglycosylation in addition to the trimming of the external chains by the increased of the enzyme treatment time (Park J.-H. et al., 2007; Takaha et al., 1998).

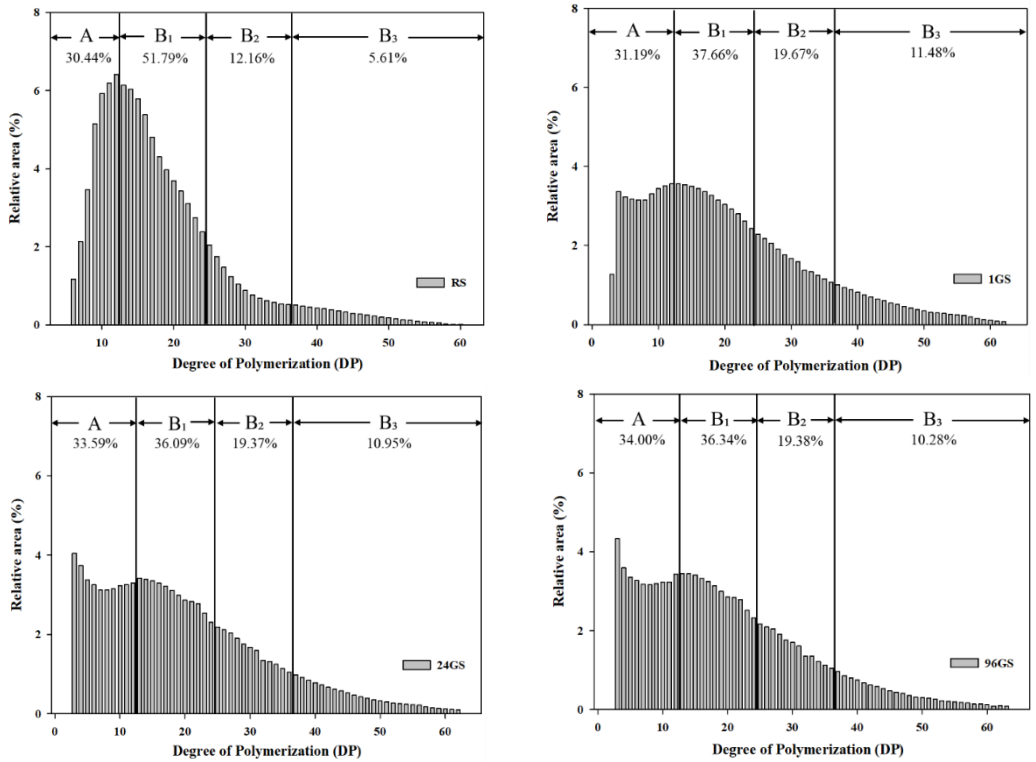


**Fig. 3. Relative branched chain length distributions of RS, 1GS, 24GS, and 96GS**

**Table 2. Rate of chain length (%) of RS, 1GS, 24GS, and 96GS**

| Host material | Chain length distribution (%) | | | |
|---|---|---|---|---|
| | A | $B_1$ | $B_2$ | $B_3$ |
| | DP≤12 | DP 13-24 | DP 25-36 | DP>36 |
| RS | 30.44 | 51.79 | 12.16 | 5.61 |
| 1GS | 31.19 | 37.66 | 19.67 | 11.48 |
| 24GS | 33.59 | 36.09 | 19.37 | 10.95 |
| 96GS | 34.00 | 36.34 | 19.38 | 10.28 |

### 5.1.3. Rheological properties

The dynamic oscillatory tests of RS, 1GS, 24GS, and 96GS (10% w/v) were estimated to determine the gelation kinetics and gel melting properties (Fig. 4-1). The gelation time ($t_c$) was defined as the sol-gel transition time at which G' (storage modulus) = G" (loss modulus), and the gel point was interpreted as the G'-G" crossover point where the sol-gel transition appeared. To interpret the gelation kinetics of the starch gels, three main parameters (G', G", and tan δ) were used. The elastic component is considered as the storage modulus (G') and the viscous component is accounted as the loss modulus (G"). The ratio of the viscous to elastic modulus (G"/G') is equal to the tangent of the phase angle (tan δ) (Zaidel et al., 2010). As exhibited in Fig. 4-1, G' and G" values of 1GS, 24GS, and 96GS were lower than those of RS before the gel time ($t_c$), indicating GS behaved a liquid-like characteristic. Then, the both modulus of GS increased gradually and intercepted, indicating the time at which the gel was formed. However, G' and G" values of GS were about one-tenth of both values of RS at the plateau. Meanwhile, RS showed the constant G' value. This is because the gelation of RS seemed to be too immediate and happened even before loading in the rheometer due to its large molecular weight, so that the gelling property were not fully identified (Lee K. Y. et al., 2008). The gel time of 1GS (996 min) was much longer than those of

24GS (452 min) and 96GS (625 min), which was due to changes in the chain length distribution over time of enzyme treatment. The gelation mechanism of GS could be suggested on the basis of impact of temperature on intermolecular interactions, which primarily contained (1) hydrogen bonding and (2) hydrophobic interactions (Rao, 2010). To explain it in more detail, first mechanism was, hydrogen bonding which was initial intermolecular local contacts including short chain segments, and secondly, hydrophobic interactions which enlarged junction zones stabilized or strengthened by van der Waals force.

The second stage (frequency sweep stage) indicated G' value of GS was considerably low and the difference between G' and G" was also low than those of RS, confirming that it showed a much weaker gel-like properties than RS (Li Y. et al., 2017; Prasad et al., 2009) (Fig. 4-2). G' is directly associated with the cross-link density of the gel network and G' is often almost same or less than 10 times larger than G" for a weak gel (StephenandPhillips, 2016). Also, tan δ (G"/G') values of RS were always less than 1, indicating that it is more elastic than viscous (YousefiandRazavi, 2015). Tan δ values of 1GS, 24GS, and 96GS were also always < 1, but they were clearly less elastic than RS because they had values close to 1 even at low frequency (0.1-1 Hz). Therefore, it could be seen that the GS represented the liquid-like characteristics.

The changes of G' values of RS gel with increasing temperature were shown

in Fig. 4-3. The values of G' maintained constant at the initial heating temperature. However, the values of G' suddenly increased at temperatures ranging from 55 to 85 ℃ (to the maximum temperature). To explain this result, DSC was measured (heating rate, 5 ℃/min; temperature range, 20-100 ℃) and the change in gel strength according to temperature was compared by increasing the temperature of RS gel. Image 2 showed that hard gel at the initial 4 ℃ exhibited a weak strength at 60 ℃, and at 80 ℃, it became stronger strength than 60℃. Freshly prepared starch gels showed that no thermal transition was observed in the temperature range of 55 to 85 ℃, the result was not by amylopectin retrogradation but by reassociation of amylose as ascribed in previous study (Matalanis et al., 2009). Kim Yujeong et al. (2012) reported that G' values of rice starch dispersion began to increase at around 55 ℃, this was due to the initiation of gelatinization of starch, which was consistent with Fig. 5. Thus, it is assumed that the increase of the G' value at above a certain temperature when the temperature of RS gel was raised again might be due to the gelatinization of ungelatinized particles in RS gel.

The melting temperature ($T_m$) was indicated at the gel-sol transition point during the heating process in which G' = G". Melting is the structural breakdown process in which disassociation of junction zones occurs. As the gels of 1GS, 24GS, and 96GS were slowly reheated to 85 ℃, the gels were completely

dissolved, which implied that the 4aGTase-treated starch formed a thermoreversible gel (Fig. 4-3). The thermoreversibility of the GS was attributed to have relatively high molecular weight amylopectin clusters with highly branched side chains with few long amylose chains (Lee K. Y. et al., 2008; Lee S. H. et al., 2008; Mun et al., 2014).

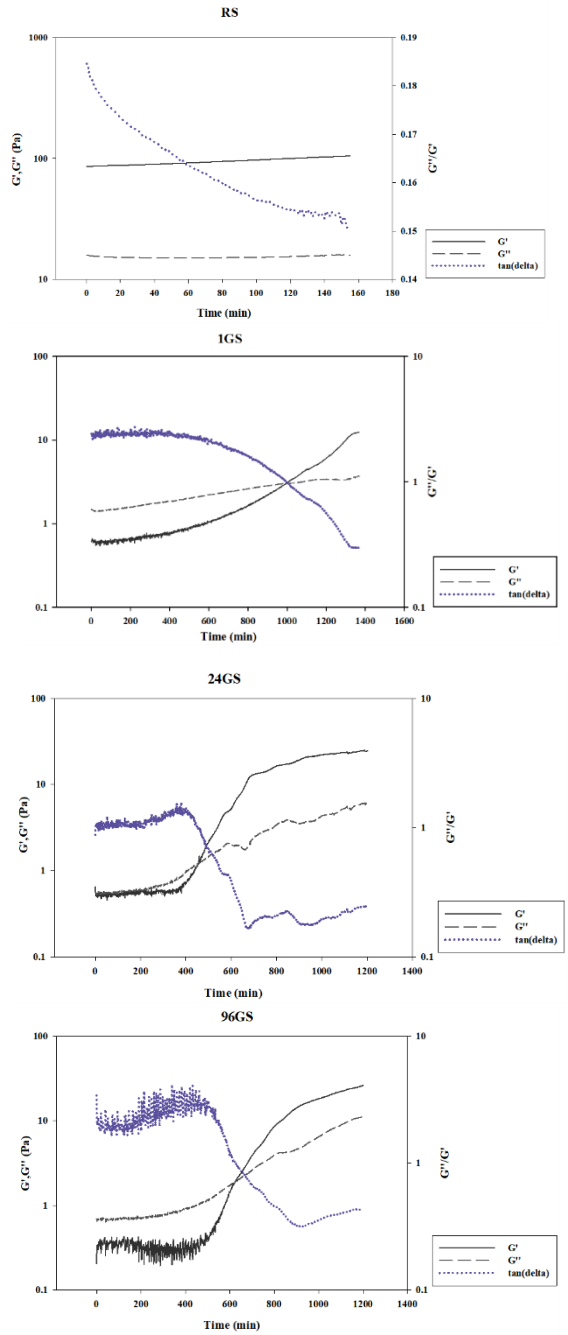


**Fig. 4-1. Time sweep measurements of RS, 1GS, 24GS, and 96GS gels**

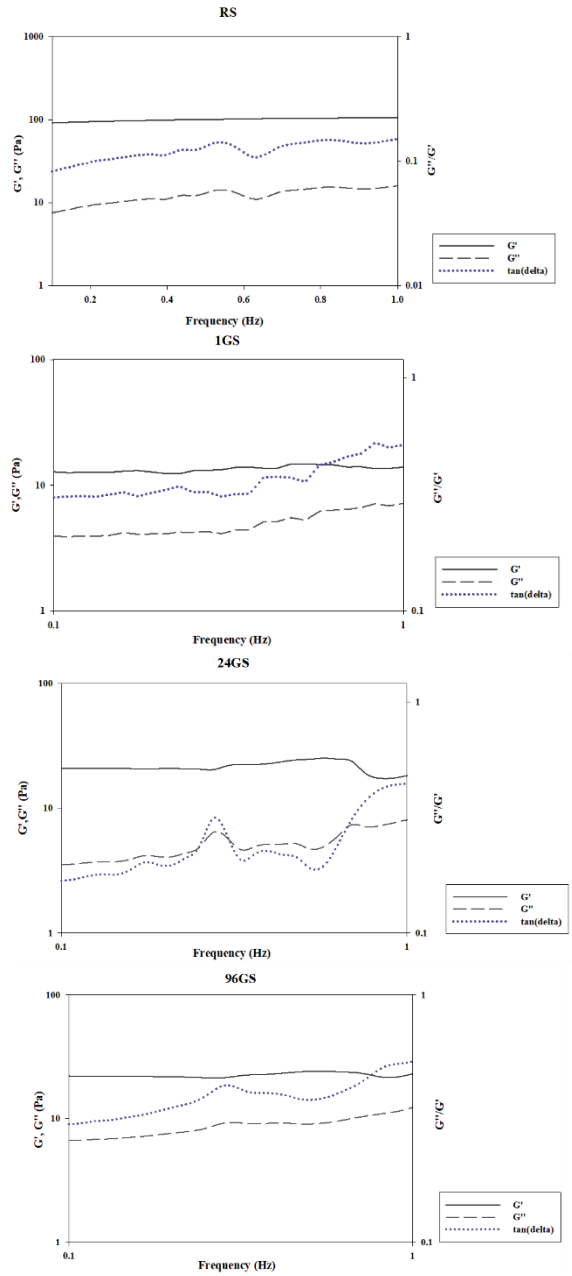


**Fig. 4-2. Frequency sweep measurements of RS, 1GS, 24GS, and 96GS gel**

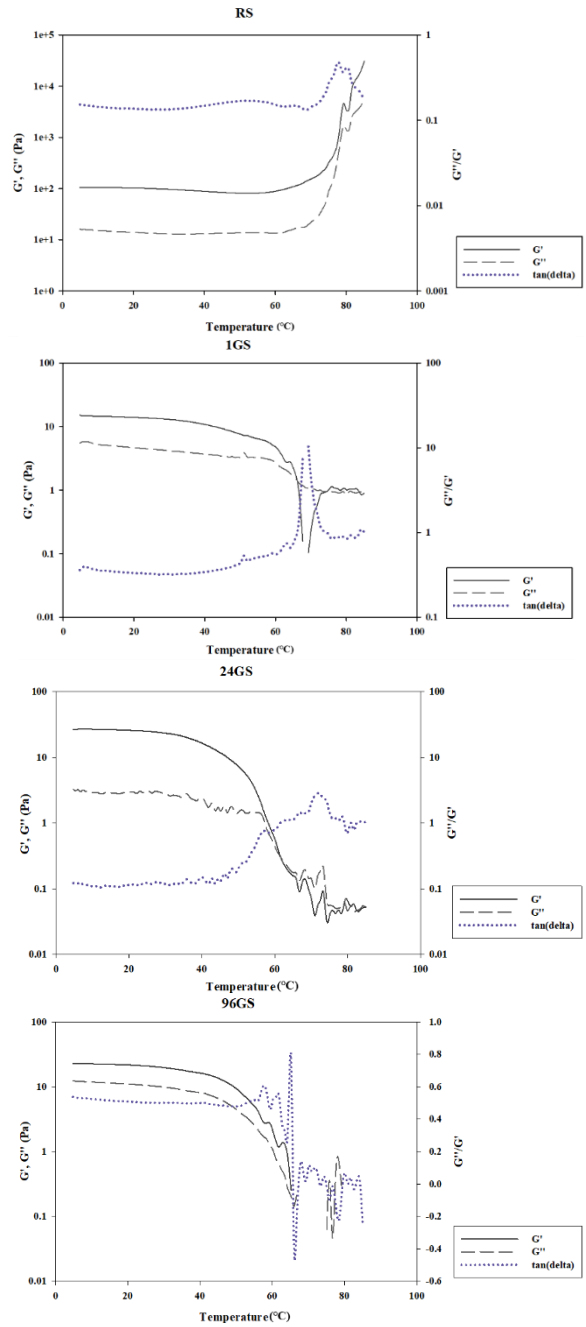


**Fig. 4-3. Temperature ramp measurements of RS, 1GS, 24GS, and 96GS gel**

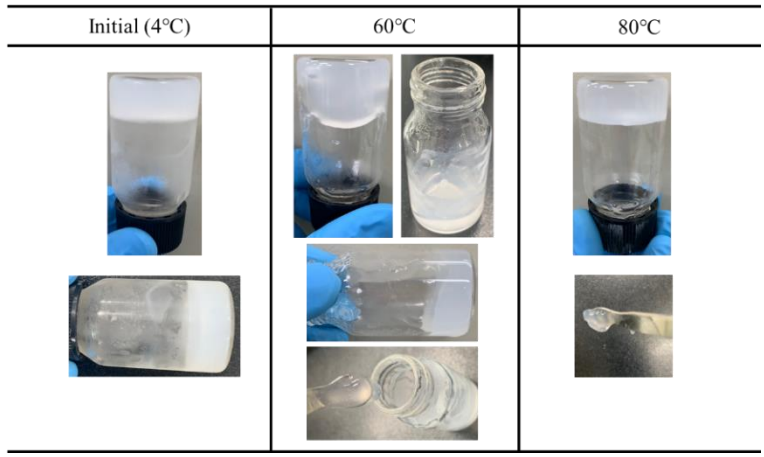


**Image 2. Visual appearance of RS gel at 4 °C, 60 °C, and 80 °C**

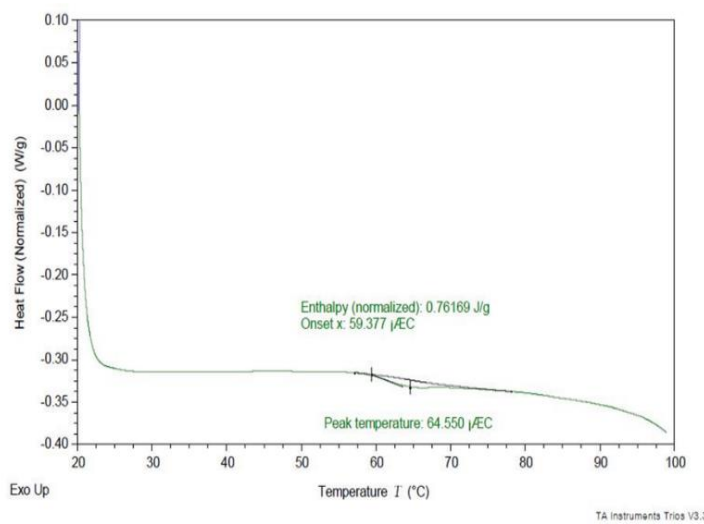


**Fig. 5. DSC thermographs of RS (heating rate: 5 °C/min; temperature range: 20-100 °C)**

### 5.1.4. Viscosity analysis

The consistency index (*K*) and flow behavior index (*n*) of the starch samples (RS, 1GS, 24GS, and 96GS) are shown in Table 3. RS showed the highest consistency index (82.40 Pa), indicating that it had gel viscosity higher than 1GS, 24GS, and 96GS ($p < 0.05$). When a shear forces was applied, it was indicated that the greater resistance was generated due to the presence of high molecular weight in gel network of RS, which appears to have resulted in an increase in viscosity. The flow behavior index (*n*) of RS was less than 1, indicating the shear-thinning behavior as consistent with previous studies (ShonandYoo, 2006; YooandYoo, 2005). Steady-state test was suggested that GS exhibited a greater Newtonian behavior because the *n* value of GS was much closer to 1 than that of RS. In other words, GS showed a decrease in viscosity due to the degradation of a large starch polymer by enzyme treatment. 1GS showed a slightly higher *K* value than 24GS and 96GS, indicating that the viscosity of GS samples decreased with increasing 4αGTase treatment time. However, there was no significant difference between 1GS, 24GS, and 96GS. The viscosity of starch is influenced by the molecular structure of amylose and amylopectin (Nakorn et al., 2009; TakoandHizukuri, 2002). In particular, high amylose content shows a positive correlation with viscosity (Xie et al., 2009). As mentioned in section 5.1.2.,

4αGTase partially extend the amylopectin branched side chain by transferring the glycosyl residue of amylose to amylopectin via intermolecular transglycosylation. It also forms cyclic glucan with low viscosity from amylose. Therefore, it is considered that the GS exhibited a lower gel viscosity than RS due to a decrease in amylose content via the molecular structural rearrangement.

**Table 3.** Consistency index (*K*) and flow behavior index (*n*) of starch samples (RS, 1GS, 24GS, and 96GS)

| | Consistency index *K* [Pa] | Flow behavior index *n* [-] | $R^2$ |
|---|---|---|---|
| RS | 82.40 ± 0.99[a] | 0.18 ± 0.02 | 0.8842 ± 0.0317 |
| 1GS | 0.13 ± 0.01[b] | 0.91 ± 0.02 | 0.9974 ± 0.0021 |
| 24GS | 0.11 ± 0.00[b] | 0.85 ± 0.01 | 0.9457 ± 0.0132 |
| 96GS | 0.09 ± 0.00[b] | 0.92 ± 0.01 | 0.9700 ± 0.0076 |

### 5.1.5. Granular morphology

The granular morphology of RS, 1GS, 24GS, and 96GS was imaged by scanning electron microscopy (SEM) (Image 3). SEM micrographs showed that RS granules had smooth surfaces and polygonal shapes with sharp angles and edges, which were in accord with the previous studies (Keeratiburana et al., 2020; Kim J. M. et al., 2010). Meanwhile, the 1GS, 24GS, and 96GS particles had spherical shapes with rough cracked surfaces. It was assumed that shapes of granules changed due to the ethanol precipitation process after enzyme treatment. In addition, GS particles were heterogeneous in size and several small particles were attached to the surrounding large particles, which might be due to the aggregation of the leached amylopectin clusters and amylose chains. The GS particles were much smaller than the RS particles, and the broken surface of the GS increased its surface area to allow it to soluble better in water.

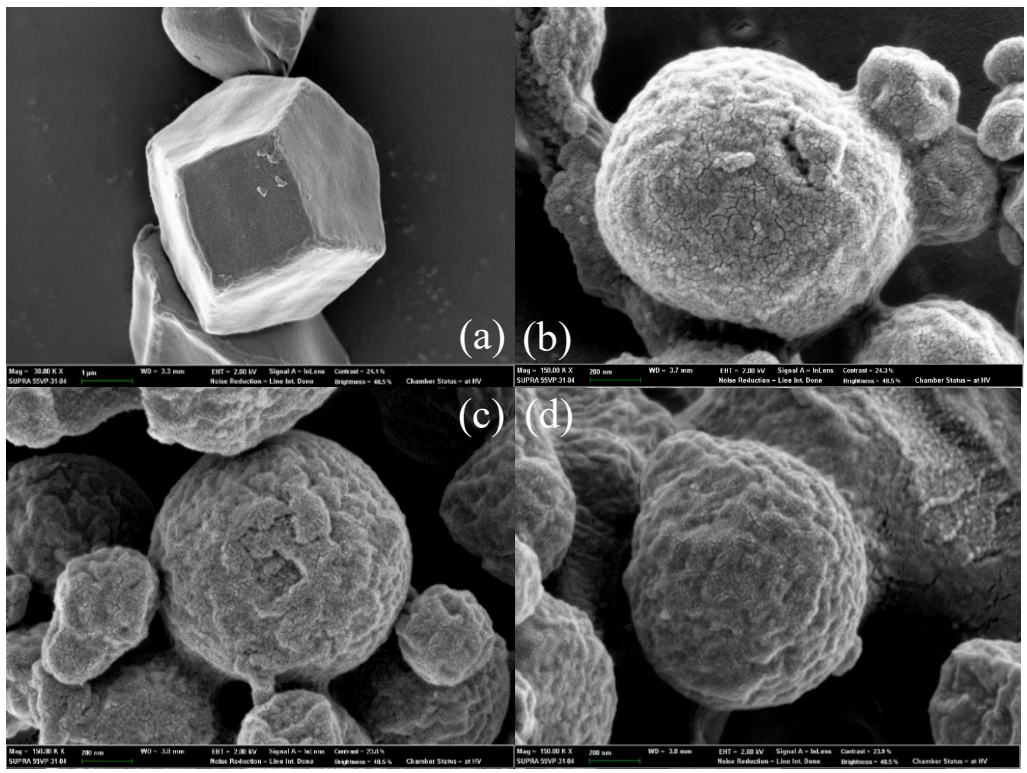


**Image 3. Scanning Electron Microscopy images of the RS, 1GS, 24GS, and 96GS (a; RS (× 30k), b; 1GS (× 150k), c; 24GS (× 150k), d; 96GS (× 150k))**

### 5.1.6. Starch crystallinity

The X-ray diffraction (XRD) patterns of RS, 1GS, 24GS, and 96GS were estimated to identify the samples with regard to starch crystallinity (Fig. 6.). Generally, natural starches can be separated into A-, B- and C- type according to their XRD patterns (CheethamandTao, 1998; Yang et al., 2020). RS showed the characteristics of A-type crystallinity, with strong diffraction peaks at approximately 15° and 23° 2θ and an unresolved doublet at about 17° and 18° 2θ, which was in conformity with the typical XRD patterns of RS (Shih et al., 2007). Meanwhile, the 1GS, 24GS, and 96GS had V-type XRD patterns with main peaks at around 13° and 20° 2θ owing to the collapsed amylose helices and formation of crystalline V-type complexes of amylose with granule fatty acids caused by the gelatinization process (Zobel et al., 1988). In the range 13-20°, GS indicated increased crystalline structure as the enzyme treatment time increased. This result was contributed to the denser packing of the crystalline structures (Kim YangandTrinh Khanh Sonand et al., 2012). Several studies have reported that the degree of granule crystallinity has a positive correlation with the amylopectin content (CheethamandTao, 1998; JenkinsandDonald, 1995). Accordingly, the increase in the crystallinity of GS indicated that the change in the distribution of branched chain length and reassignment of amylopectin caused by enzyme

treatment reduced amorphous region and increased crystalline region (Kim YangandKim Young-Limand et al., 2012).

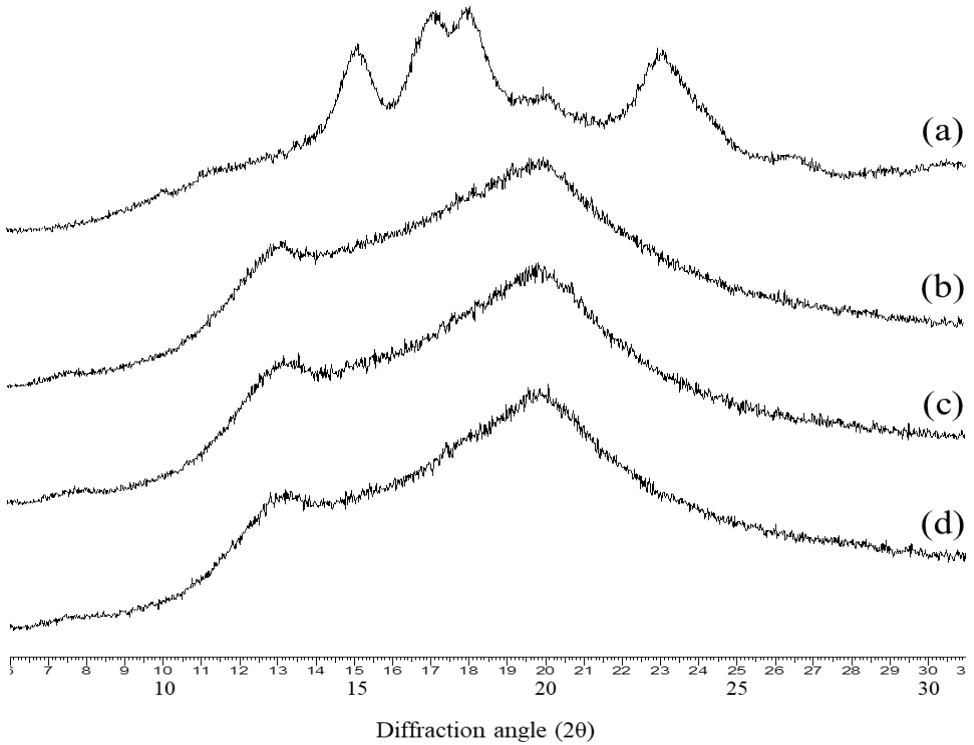


**Fig. 6. X-ray diffraction pattern of (a) RS, (b) 1GS, (c) 24GS, and (d) 96GS**

### 5.1.7. Iodine absorption capacity

The iodine absorption capacity of RS, 1GS, 24GS, and 96GS is shown in Fig. 7 and Image 4. The color of amylose standard-iodine complex was a deep blue color, with the highest absorbance occurring at a peak wavelength of 625 nm, which is consistent with previous studies (Bates et al., 1943; ImmelandLichtenthaler, 2000; SaibeneandSeetharaman, 2006). The reason for this blue color was that iodine formed the complex with helical structure of amylose. On the other hand, the iodine could also slightly form a complex with amylopectin, which appeared light purple color. The peak wavelength of RS ($\lambda_{max} \approx$ 592nm) was in the middle of the peak wavelength of amylose and amylopectin, it might that both components were incorporated in iodine complexation. 1GS, 24GS, and 96GS had a deep violet color with a leftward shift of the wavelength ($\lambda_{max} \approx$ 550nm). The alteration of absorbance of iodine-polysaccharide complexes has been reported that it can be regarded as an indicator of a change in the composition of linear or branched fraction of starch molecules (KaurandSingh, 2000). In addition, the color of amylose-iodine complex changes depending on the degree of polymerization (DP) of the amylose helix (brown, DP 21-24; red, DP 25-29; red-violet, DP 30-38; blue violet, DP 39-46; blue, DP > 47) (SaibeneandSeetharaman, 2006). Thus, the result might be

attributed to an increase in the number of molecules with DP 30-48 as a result of intermolecular transglycosylation by enzyme treatment (Do et al., 2012). Furthermore, 24GS and 96GS indicated higher absorbance than 1GS. The increased iodine absorption capacity of 24GS and 96GS may be ascribed to the increased number of longer side chains and the formation of cyclic glucans by intramolecular transglycosylation (Do et al., 2012).

**Image 4. Appearance of color change of RS, 1GS, 24GS, 96GS, amylose, and amylopectin reacted with iodine solution**

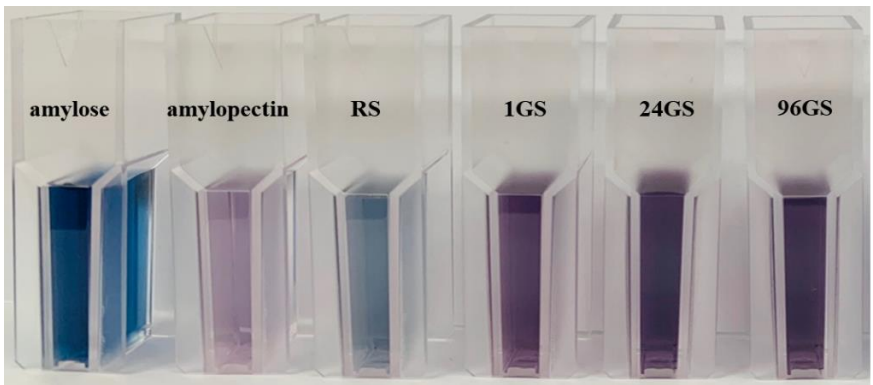


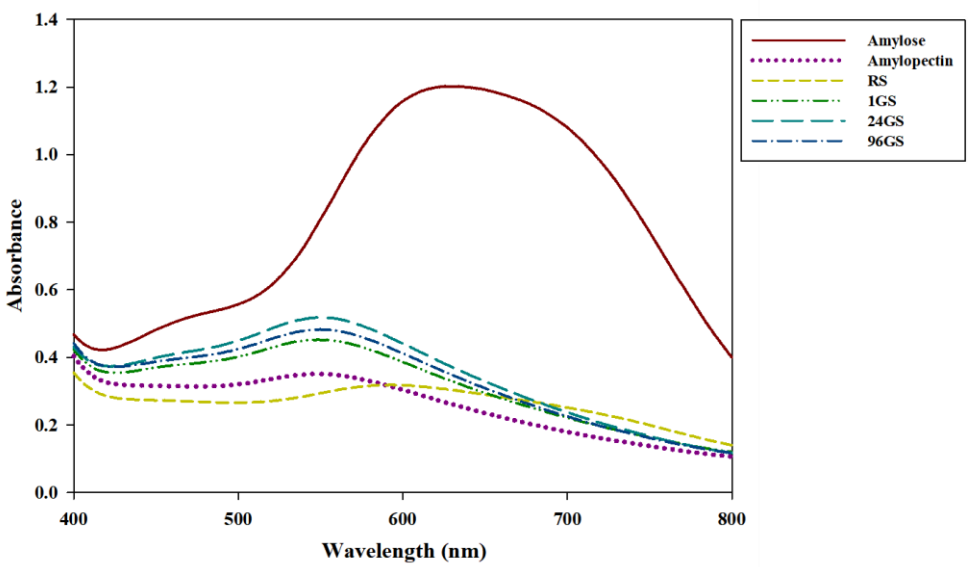


**Fig. 7. Spectra of iodine absorbance of RS, 1GS, 24GS, 96GS, amylose, and amylopectin**

## 5.2. Encapsulation of the curcumin in filled hydrogel & micro-encapsulation powder

### 5.2.1. Characteristics of filled hydrogel

#### 5.2.1.1. Rheological properties of filled hydrogel

Since the storage modulus (G') and loss modulus (G") are the main parameters in characterizing the viscoelastic properties of semi-solid hydrogels, dynamic oscillatory tests were evaluated to analyze the dynamic rheological properties of FH samples (RS-FH, 1GS-FH, 24GS-FH, and 96GS-FH) (Fig. 8). Based on the dynamic moduli (G' and G"), GS-FH showed that the G' value was considerably low and the difference between G' and G" was also low (G' was 2-3 times larger than G"), confirming that it exhibited a much weaker the gel-like properties than RS-FH (Li Y. et al., 2017; Prasad et al., 2009). G' is directly associated with the cross-link density of the gel network and G’ is often almost same or less than 10 times larger than G" for a weak gel (StephenandPhillips, 2016). Also, tan δ (G"/G') values of RS-FH were always less than 1, indicating that it is more elastic than viscous (YousefiandRazavi, 2015). Values of 1GS-FH, 24GS-FH, and 96GS-FH were also always < 1, but they were clearly less elastic than RS-FH because they had values close to 1 even at low frequency (0.1-1 Hz). Therefore, it could be seen that the GS-FH samples (1GS-FH, 24GS-FH, and 96GS-FH) represented

the liquid-like characteristics. As described above, this may be because the molecular structure of GS samples were rearranged by enzyme treatment, which could not form a rigid gel structure. Among GS samples, there was no significant differences in all parameters. It was assumed that the difference was not noticeable because the G' and G" absolute values of 1GS-FH, 24GS-FH, and 96GS-FH were greatly small to indicate a distinct difference compared to the gel strength of RS-FH composed of native rice starch (Li Y. et al., 2017).

Viscosity is the resistance of a fluid against any irreversible positional change of its volume elements (Schramm, 1994). The consistency index ($K$) and flow behavior index ($n$) of the filled hydrogel samples (RS-FH, 1GS-FH, 24GS-FH, and 96GS-FH) and EM were shown in Table 4. The tendency was similar when comparing $K$ and $n$ values of the filled hydrogel samples with the starch samples. RS-FH showed the highest consistency index (132.10 Pa), and had gel viscosity higher than EM, 1GS-FH, 24GS-FH, and 96GS-FH ($p < 0.05$), which was attributed to the influence of high molecular weight in gel network of RS-FH as mentioned above (section 5.1.4). Since the consistency index ($n$) of EM and GS-FH samples showed no significant difference and GS-FH samples were much closer to 1 than that of RS-FH, GS-FHs, like EM with liquid properties, indicated a Newtonian behavior. This result was ascribed to the hydrolysis of a large starch

polymer by enzyme treatment. Among GS-FH samples, 1GS-FH exhibited a slightly higher *K* value than 24GS-FH and 96GS-FH, which might be due to its increased intramolecular friction and larger molecular weight (Jiang et al., 2014). Meanwhile, the *K* values of the FH systems were much higher than that of only starch samples. Based on this finding, it was assumed that the interaction between oil and starch molecules caused an increase in viscosity.

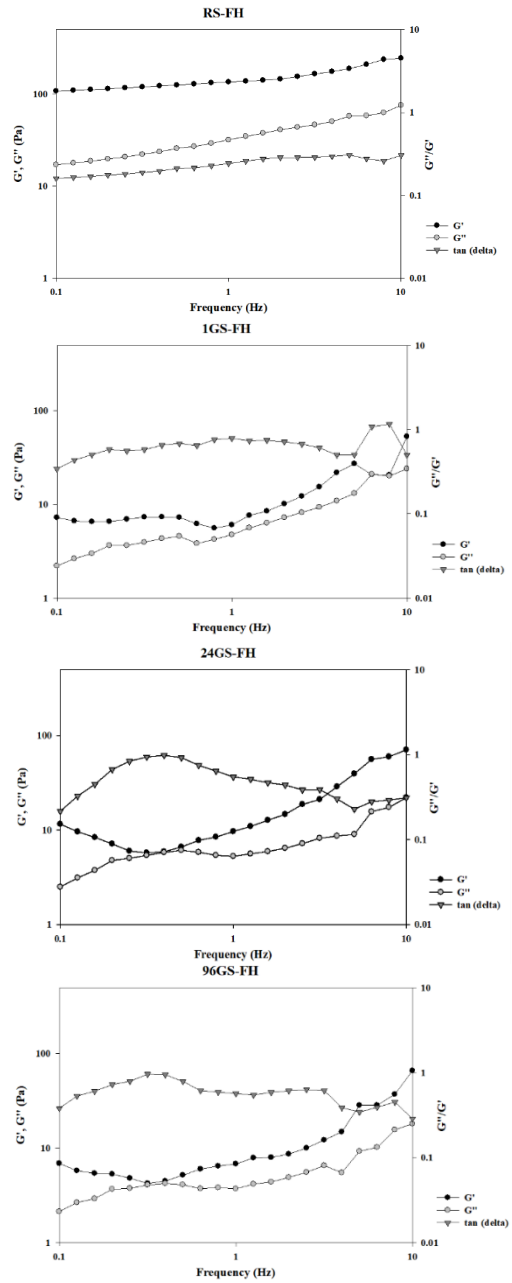


**Fig. 8. Rheological properties of filled hydrogel samples (RS-FH, 1GS-FH, 24GS-FH, and 96GS-FH) during a frequency sweep at 25°C.**

**Table 4. Consistency index (*K*) and flow behavior index (*n*) of filled hydrogel samples (EM, RS-FH, 1GS-FH, 24GS-FH, and 96GS-FH)**

| | Consistency index *K* [Pa] | Flow behavior index *n* [-] | $R^2$ |
|---|---|---|---|
| EM | $0.09 \pm 0.01^{a}$ | $0.91 \pm 0.05$ | $0.8826 \pm 0.0508$ |
| RS-FH | $132.10 \pm 6.75^{b}$ | $0.18 \pm 0.03$ | $0.9565 \pm 0.0091$ |
| 1GS-FH | $0.35 \pm 0.02^{a}$ | $0.77 \pm 0.09$ | $0.9564 \pm 0.0449$ |
| 24GS-FH | $0.18 \pm 0.08^{a}$ | $0.79 \pm 0.15$ | $0.9856 \pm 0.0155$ |
| 96GS-FH | $0.23 \pm 0.02^{a}$ | $0.71 \pm 0.06$ | $0.9491 \pm 0.0320$ |

### 5.2.1.2. Texture profile analysis (TPA)

Texture profile analysis (TPA) was performed to compare the textural properties of the filled hydrogel samples, and the mean values of the textural parameters are shown in Table 5. The hardness showed a significant difference among FH samples and markedly decreased in 96GS-FH. The gumminess (hardness × cohesiveness) and chewiness (hardness × cohesiveness × springiness), which are mainly affected by hardness, also resulted in statistically low situations at 96GS-FH. These results might be attributed to changes in the amylose and amylopectin structure of GS caused by enzyme treatment. As described in the results of HPSEC and HPAEC, the amylose molecules of 1GS, 24GS, and 96GS were hydrolyzed, and the ratio of amylopectin with a longer branched chain length distribution (DP > 25) increased due to enzyme reaction (Figs. 2 and 3). In particular, the average DP value of 96GS amylose region (approx. DP 130) was also significantly lower than that of RS (approx. DP 980-1110) (Amagliani et al., 2016). As can be seen in Image 5, visual appearances of GS-FH samples showed that their strengths of gels were noticeably weaker than RS-FH. Previous study reported that the high hardness in the RS was related to high amylose contents leading to the crystallization in a short period of time (Kong et al., 2015). The amylose content in rice starch by 4αGTase treatment not only decreased

remarkable, but also the proportion of amylose size and even smaller molecules was huge increased (Cho et al., 2009). Therefore, 96GS formed a weak gel due to a significantly low molecular weight, which was considered to show a relatively low hardness. Other parameters, adhesiveness and elasticity, were not significantly different among FH samples.

**Table 5. Textural properties of filled hydrogel (RS-FH, 1GS-FH, 24GS-FH, and 96GS-FH)**

| FH sample | Gel characteristics | | | | | |
|---|---|---|---|---|---|---|
| | Hardness [N] | Adhesiveness | Cohesiveness | Springiness (%) | Gumminess [N] | Chewiness [N] |
| RS-FH | $5.17 \pm 0.10^{d}$ | $- 1.56 \pm 0.07^{a}$ | $0.68 \pm 0.02^{b}$ | $93.53 \pm 0.27^{a}$ | $3.52 \pm 0.17^{c}$ | $329.45 \pm 14.91^{c}$ |
| 1GS-FH | $4.10 \pm 0.05^{c}$ | $- 1.80 \pm 0.28^{a}$ | $0.35 \pm 0.01^{a}$ | $94.66 \pm 11.34^{a}$ | $1.45 \pm 0.08^{b}$ | $136.90 \pm 9.21^{b}$ |
| 24GS-FH | $1.81 \pm 0.13^{b}$ | $- 2.00 \pm 0.12^{a}$ | $0.39 \pm 0.02^{a}$ | $88.87 \pm 0.68^{a}$ | $0.70 \pm 0.01^{a}$ | $62.49 \pm 1.05^{a}$ |
| 96GS-FH | $1.18 \pm 0.13^{a}$ | $- 1.75 \pm 0.20^{a}$ | $0.43 \pm 0.04^{a}$ | $86.91 \pm 2.47^{a}$ | $0.50 \pm 0.00^{a}$ | $43.56 \pm 1.06^{a}$ |

**Image 5. Visual appearance of filled hydrogels (RS-FH, 1GS-FH, 24GS-FH, and 96GS-FH)**

### 5.2.2. Characteristics of microencapsulation powder

#### 5.2.2.1. Morphology of microencapsulation powder

The morphology of curcumin, starch samples (RS, 1GS, 24GS, and 96GS), and powder samples (EMP, RS-FHP, 1GS-FHP, 24GS-FHP, 96GS-FHP) were observed by SEM (Image 6). Curcumin exhibited rod-like long particles, and its size was comparable to that of GS. The freeze-drying powder samples had relatively larger particles than starch samples. Moreover, it had flat surfaces and resembled flakes, confirming the shapes previously mentioned by several studies (AnwarandKunz, 2011; KaushikandRoos, 2007; Sousdaleff et al., 2013). Especially, porous structures on the surface of all powder samples were formed by sublimation of ice crystals during the freeze-drying process (Cano-Higuita et al., 2015). This result was possibly caused by destabilization of the emulsion during the freezing process, to be more specific, ice crystals formed in the aqueous phase of emulsion without starch when emulsion was stored at –20℃, which penetrated the oil droplets and interrupted their interfacial (Fioramonti et al., 2017). This latter would accelerate coalescence and releasing of the oil from the core to the surface (Fioramonti et al., 2017). Meanwhile, the holes in EMP and RS-FHP were larger in size and number than GS-FHP samples.

In the case of EMP manufactured without starch, the powder seemed deep

yellow color and somewhat lumpy as shown in its visual appearance (Image 7). This was due to more surface oil in emulsion without starch than other powders prepared with RS or GS, which made the powder observed agglomerated (No et al.). On the other hand, RS-FHP and GS-FHP were of relatively small powder masses. Furthermore, the color was gradually lighter when polymers were added to an emulsion system. The degree of lightening in color was depending on the type of polymers (RS, 1GS, 24GS, and 96GS). The original deep yellow color disappeared when RS was added, while the color maintained at an appropriate level when GS samples were added. Color difference was no noticeable among GS-FHP samples. Based on the SEM data above, on the premise that all powder samples had some degree of destabilization of emulsion during the freeze-drying process, this result might be because the addition of RS masked the yellow color shown by free oil leaking to the surface of the particles to some extent (Fioramonti et al., 2017; No et al.). Meanwhile, in case of GS, yellowish color seemed to be maintained, which was thought to be due to molecular weight of GS. It had a relatively small molecular weight compared to RS, which would make up the gel network on the oil surface relatively thin. Therefore, it would not have completely covered the color of the oil, which represented yellow.

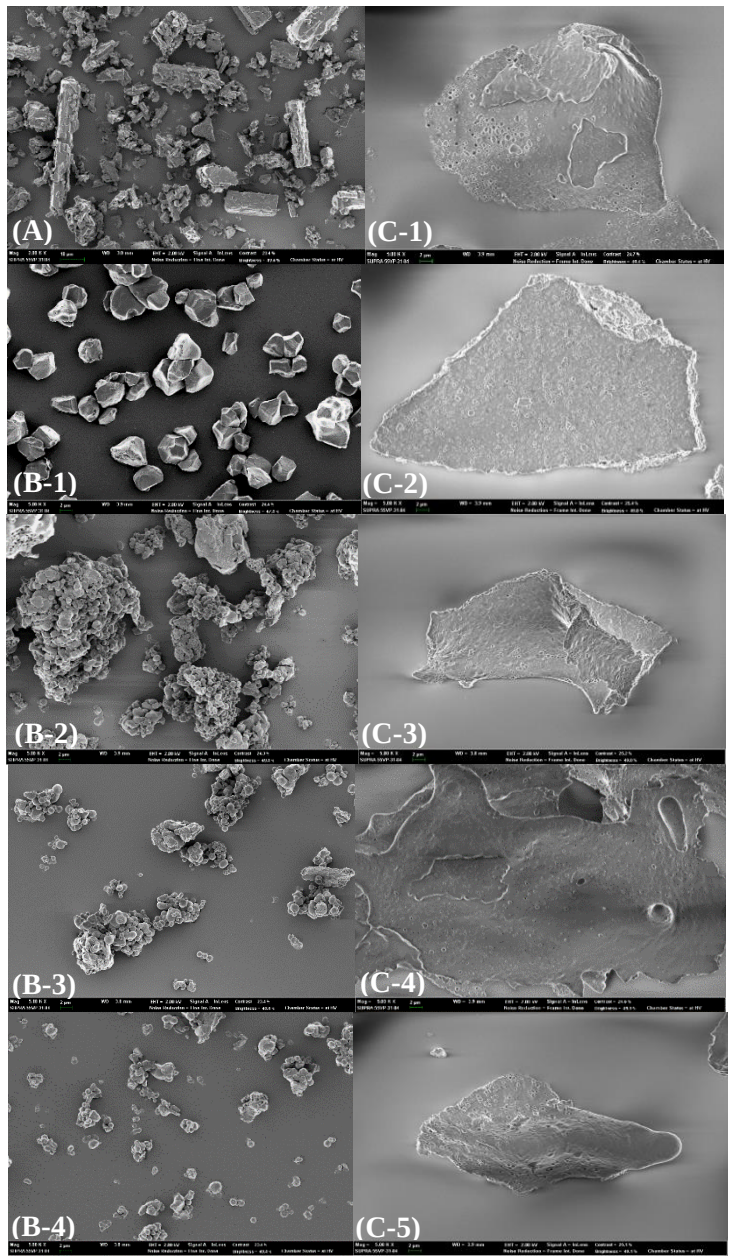


**Image 6. Scanning Electron Microscopy images of (A) curcumin; (B-1) RS, (B-2) 1GS, (B-3) 24GS, (B-4) 96GS; (C-1) EMP, (C-2) RS-FHP, (C-3) 1GS-FHP, (C-4) 24GS-FHP, (C-5) 96GS-FHP (A, × 2K; B-1~B-4, C-1~C-5, × 5K)**


**Image 7. Visual appearance of the EMP, RS-FH, 1GS-FH, 24GS-FH, and 96GS-FH**

### 5.2.2.2. Fourier Transform Infrared Spectroscopy (FT-IR)

The FR-IR spectra of Cur, starch samples (RS, 1GS, 24GS, and 96GS), EMP, physical mixture (EMP + starch samples), and FHP (RS-FHP, 1GS-FHP, 24GS-FHP, and 96GS-FHP) are shown in Fig. 9a and b to explain potential interactions among curcumin, emulsion, and starch. In the spectrum of curcumin, a broad peak at about 3502 $cm^{-1}$, which was attributed to —OH stretching on the benzene ring (Li J.andShinand et al., 2016). In addition, 1625 $cm^{-1}$ was determined as the combined peak of vibration of C═C and C═O; 1498 $cm^{-1}$ of peak was C—O and C—C vibrations; peak at 1270 $cm^{-1}$ was aromatic C—O stretching vibration, and 1026 $cm^{-1}$ was C—O—C stretching vibrations (Mohan et al., 2012). The sharp absorption bands at 1026 $cm^{-1}$ and 856 $cm^{-1}$ exhibited C—O—C stretching; the band at 956 $cm^{-1}$ was identified to be benzoate trans —CH (Park H. R. et al., 2019).

The spectra of EMP encapsulated curcumin was similar to those of WPI and soybean oil, unlike Cur. A previous study reported that the major peaks (3272 $cm^{-1}$, 2944 $cm^{-1}$, 1630 $cm^{-1}$, 1520 $cm^{-1}$) indicated on the WPI spectra Mohammadian et al. (2019). In this study, the peaks of EMP could be also observed in wavenumber similar to a previous study (3286 $cm^{-1}$, 2924 $cm^{-1}$, 1643 $cm^{-1}$, 1537

$cm^{-1}$). The intensity of 1643 $cm^{-1}$ referred to C—O stretching vibration and 1537 $cm^{-1}$ referred to C—N stretching, which is characterized by amide I band and amide II band, respectively (GhaleshahiandRajabzadeh, 2020; Zhang Zeyu et al., 2017). Meanwhile, the remaining peaks of the EMP that did not overlap the spectra of WPI were 2854 $cm^{-1}$, 1743 $cm^{-1}$, 1159 $cm^{-1}$. It was the peak of the soybean oil contained in emulsions, representing —$CH_2$, —C═O, and C—O—C, respectively (Qiu et al., 2011).

The spectra of physical mixtures (e.g. EMP with starch samples) were mostly combinations of the peaks from EMP and starch samples. The major peaks belonging to EMP were mainly observed in the spectra of the physical mixtures (2924 $cm^{-1}$, 2854 $cm^{-1}$, 1743 $cm^{-1}$, 1643 $cm^{-1}$, 1159 $cm^{-1}$, 600 $cm^{-1}$). Meanwhile, FHP (RS-FHP, 1GS-FHP, 24GS-FHP, and 96GS-FHP) samples were also shown to be similar to the spectra of their physical mixtures. It was assumed that the result was due to the absence of chemical interaction between emulsion and starch in the manufacturing process of FHP and simply to the physical barrier of starch surrounding the oil droplets.

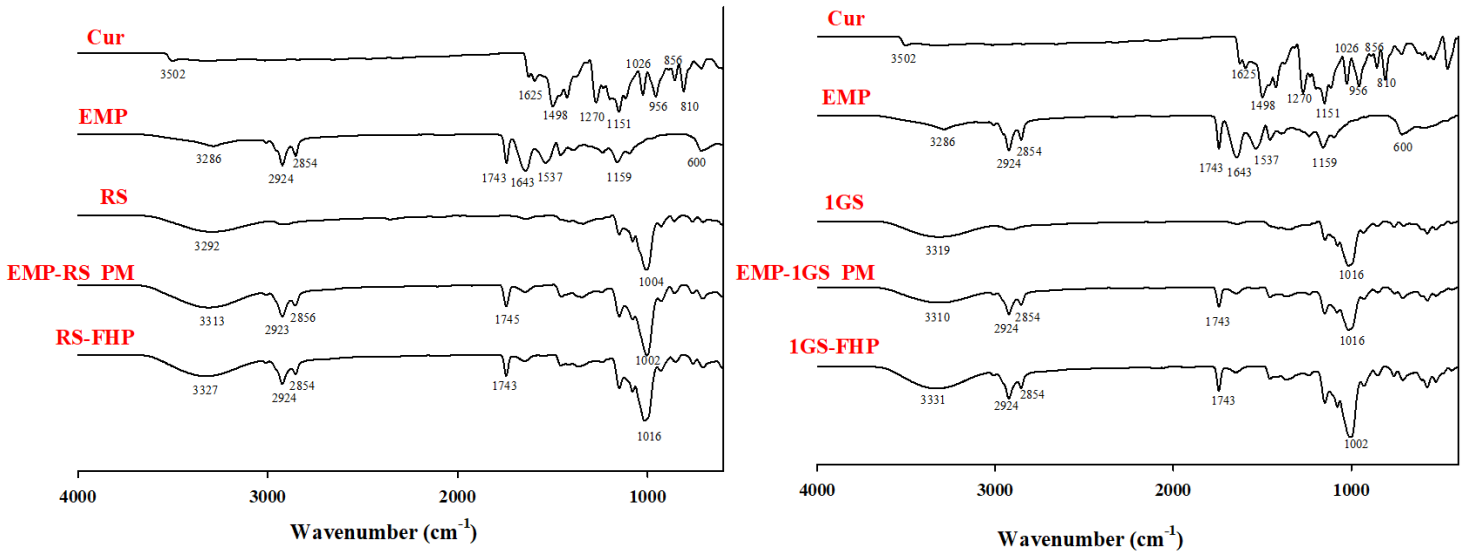


**Fig. 9. (a) FT-IR spectra of Cur, EMP, starch (RS and 1GS), physical mixtures (-PM), and FH powder (-FHP)**

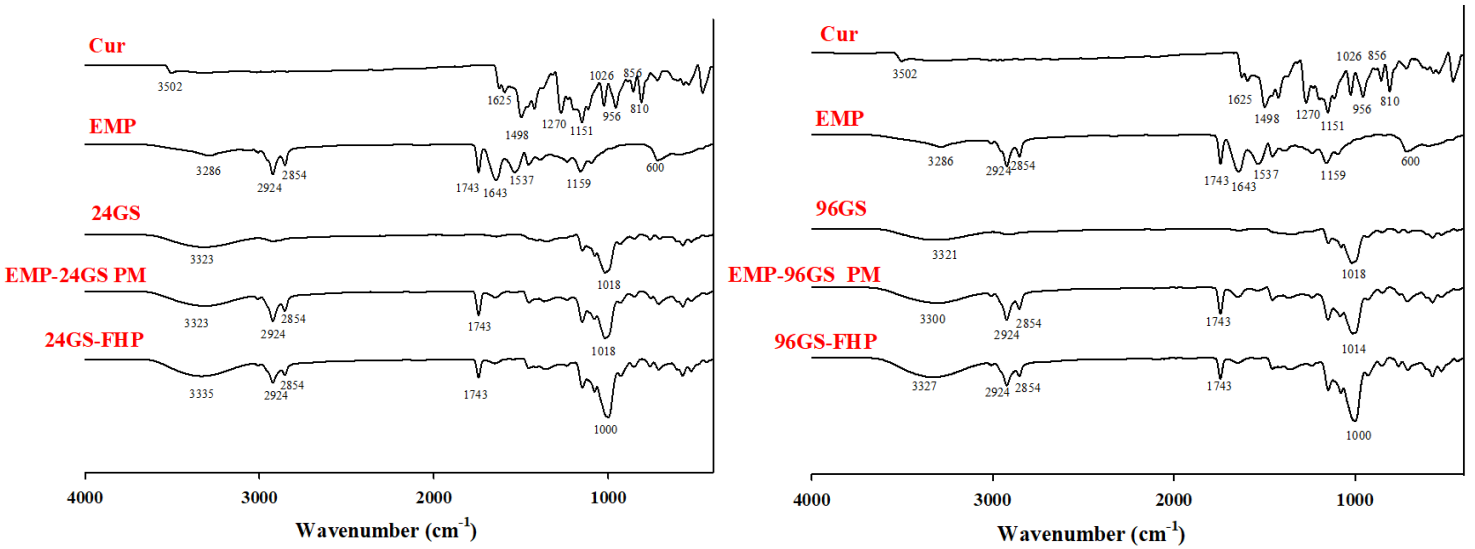


**Fig. 9. (b) FT-IR spectra of Cur, EMP, starch (24GS and 96GS), physical mixtures (-PM), and FH powder (-FHP)**

### 5.2.3. Curcumin stability analysis of filled hydrogel and micro-encapsulation powder

#### 5.2.3.1. Heat stability

Heat stability of curcumin is an important matter during their processing and applications, such as cooking and heat sterilization (Li Z.-l. et al., 2018). The effects of EM and FH systems on the heat stability of curcumin were evaluated by measuring the curcumin retention (%) after heat treatment at 95 ℃ for 24h (Fig. 10a and b). The amount of retained curcumin of all samples sharply decreased to less than 50 percent within two hours. Previous studies reported that emulsion was unstable to aggregation of the particles at elevated temperature due to the denaturation of whey protein which causes aggregation (Qian et al., 2012b; Sun et al., 2017). On the other hand, heat stability of emulsion with proteins and polysaccharides was improved due to their excellent surface active properties and ability of providing a stabilization effect via viscosity modification or gelation of the continuous phase of emulsion, respectively (Dickinson, 2003; Dickinson, 2009). Therefore, EM had been expected to have the lowest heat stability before the experiment. However, as shown in Fig. 10a, EM indicated the highest level of protective effect with higher curcumin retention (> 17.72%) at all times, which was contrary to the expected outcome. It was assumed that these results were attributed to the physical difference between emulsions corresponding to liquids

and FH corresponding to semi-sold gels. In general, the thermal conductivity of liquids is well known to be lower than that of solids. Therefore, it was suggested that the properties of samples close to liquid characteristics had higher heat stability, which decreased curcumin decomposition less at 95 ℃.

Generally, modification of curcumin may occur shift of the double bonds, degradation to lower molecular weight compounds, such as ferulic acid, vanillin and vanillic acid during heat treatment, exhibiting a susceptibility of the 'diketone bridge' of curcumin to heat (Suresh et al., 2009).

Meanwhile, the trend in curcumin retention of samples up to 3h indicated significantly difference in order of EM, GS-FH, RS-FH. The retention of RS-FH decreased rapidly within the first 10 min and was about 5.68% after 30 min. GS-FH showed a similar the value of curcumin retention about 17.27% on average among themselves after 30 min, which had an approximately increased 3.04-fold of heat stability of curcumin than that of RS-FH. Among reconstituted EM and FH samples, the levels of all FH' samples became almost similar, which was about 4.01 times less than EM within the first 30 min.

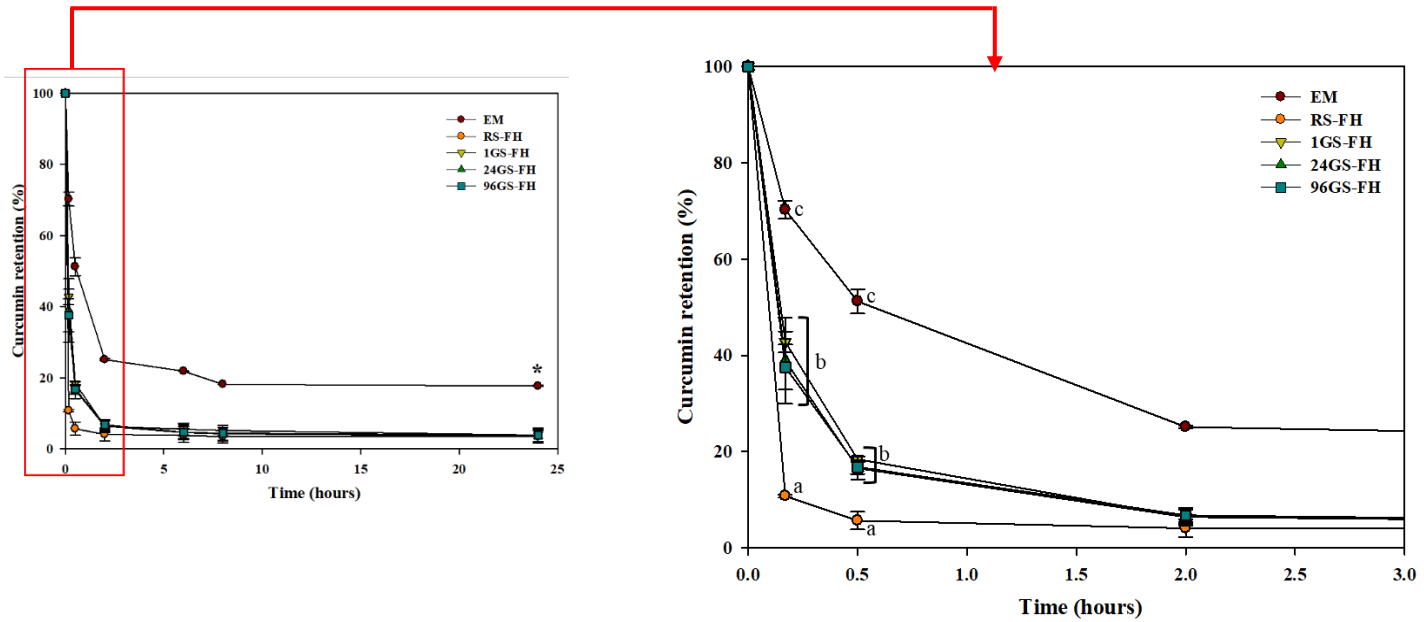


**Fig. 10. (a) Retention rate (%) of curcumin encapsulated with EM, RS-FH, 1GS-FH, 24GS-FH, and 96GS-FH. [a] Results marked with the different letter in each time zones are significantly different ($p < 0.05$). (left: after heated for 24h, right: partial section during heating from 0 to 3h)**

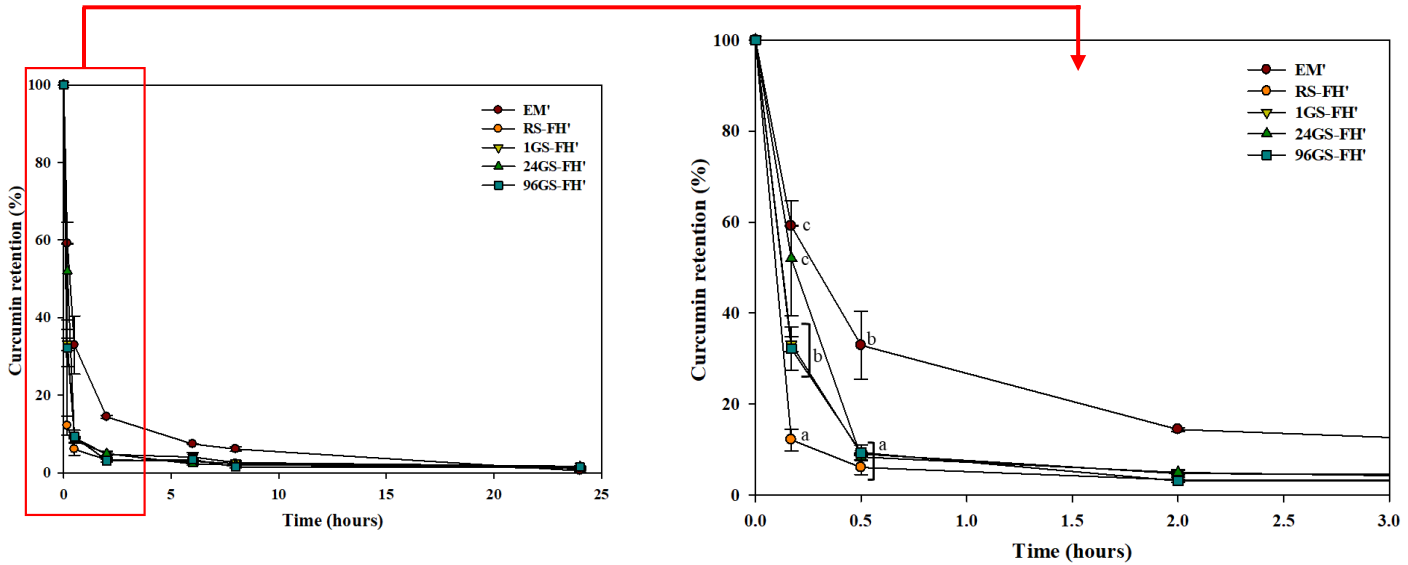


**Fig. 10. (b) Retention rate (%) of curcumin encapsulated with EM', RS-FH', 1GS-FH', 24GS-FH', and 96GS-FH'. [a] Results marked with the different letter in each time zones are significantly different ($p < 0.05$). (left: after heated for 24h, right: partial section during heating from 0 to 3h)**

### 5.2.3.2. UV stability

Curcumin is very unstable to UV irradiation which is a simple and effective sterilization method during food and beverage processing (Dai et al., 2018). Therefore, in this study, the UV stability of curcumin encapsulated in EM, RS-FH, 1GS-FH, 24GS-FH, and 96GS-FH was estimated. Curcumin protection effect of GS-FH was evaluated by measuring the curcumin retention (%) after UVB exposure for 7 h, and the results were compared with EM and RS-FH. In addition, EM', RS-FH', 1GS-FH', 24GS-FH', and 96GS-FH' were also measured for UV stability under the same conditions. As shown in Fig. 11a, the amount of remained curcumin of all samples gradually decreased as the UV irradiation time was extended. FH was more stable against UV irradiation at all times than EM. After 7 h of UV irradiation, curcumin in EM was destroyed by approx. 60%, while curcumin in FH was retained more than 50%. Curcumin has a 2-hydroxy methoxy phenyl ring linked by 2-β-diketone groups, making it unstable to UV (Lee B. H. et al., 2013). Curcumin, when exposed to UV radiation in both solution and solid state, mainly loss of two hydrogen atoms to form a cyclization product of curcumin (Tønnesen et al., 1986). Degraded curcumin acts as a photosensitizer of singlet oxygen and undergoes self-sensitized decomposition. Previous study reported that several radicals induced by UV irradiation in the emulsion system

may oxidize or react with the charged groups, and neutralized the charge distributed on the interface of lipid droplets of emulsion, thereby deteriorating stability (Li J.andHwangand et al., 2016). In addition, they also revealed that coating the emulsion with polymers could more effectively protect curcumin from oxidation and degradation. Therefore, the FH used in this study might also due to the protection of curcumin by providing a physical barrier to block the passage of UV rays (Glaze et al., 1995; Li J.andHwangand et al., 2016).

Among FH, RS-FH showed the highest level of protective effect with higher curcumin retention (> 72.6%). This may be due to the fact that RS has a faster gelation rate at room temperature, forming a harder gel network than GS, thereby increasing the UV blocking effect. GS-FH (approx. 1GS > 53.3%; 96GS > 60.3%) also showed significant curcumin protection effect against UV. GS was initially maintained in a liquid state during preparation, but with time, the solution has the unique rheological properties that forms a gel (Lee K. Y. et al., 2006; Park J.-H. et al., 2007). Therefore, this result might be due to GS forming a gel network in the O/W emulsion itself preventing the release of curcumin existing therein. Previous studies reported that the possibility of using emulsifiers in emulsions of starch and/or enzymatically modified starch as gelling polymers (Kasprzak et al., 2018; Mun et al., 2011). They found that when the enzymatically modified starch

was included in the W/O/W internal water phase, the encapsulation efficiency and stability of emulsion could be improved while reducing the average diameter of the oil phase. They also suggested the possibility of the clean label emulsion formulation in the food industry by stabilizing the microstructure of the emulsion by the wax starch.

Meanwhile, 96GS-FH (approx. 60.3%) had a significantly higher curcumin protection than 1GS-FH (approx. 53.3%). In the molecular weight distribution diagram of GS (Fig. 2), 96GS was composed of amylopectin clusters and a more uniform molecular weight distribution than 1GS. Therefore, 96GS gel might have formed a well-organized and dense physical barriers, thereby increasing the protective effect of curcumin as in the our previous study (Park H. R. et al., 2019). Among reconstituted EM and FH samples, the UV stability of RS-FH' and 1GS-FH', which had relatively large molecular weight, was significantly higher than that of EM', 24GS-FH', and 96GS-FH'. They had a 1.45- and 2.04-fold UV stability of curcumin than EM (control), respectively. Our results suggested that GS-FH as well as RS-FH could be used as a potential well materials to improve the stability of curcumin from UV, thereby extending shelf-life during storage.

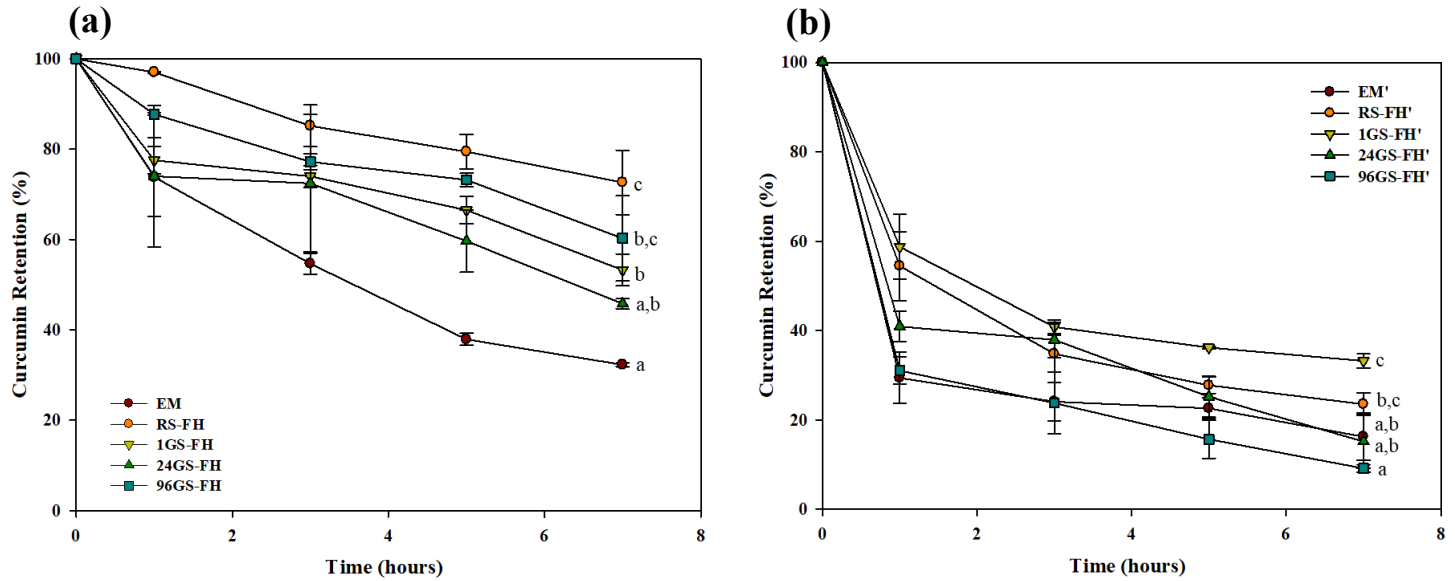


**Fig. 11. Retention rate (%) of curcumin encapsulated with (a) EM, RS-FH, 1GS-FH, 24GS-FH, and 96GS-FH (b) EM', RS-FH', 1GS-FH', 24GS-FH', and 96GS-FH' after UVB exposure for 7h.**

### 5.2.4. Curcumin retention rate & bioavailability analysis of curcumin in filled hydrogel and microencapsulation powder

#### 5.2.4.1. *In vitro* digestibility test

The rate and extent of lipid digestion was determined by using the pH stat measurement. The lipid digestibility was measured by titrating the volume of NaOH to maintain a constant pH 7.0 after adding artificial intestinal fluids during the 120 min of intestinal digestion, and then calculating the fraction of free fatty acid (FFA) released from the mixture. As a result, the volume of NaOH solution added in all samples increased rapidly during the first 10 min, followed by a more progressive increase at longer times (Fig. 12a and b). The reason for the early addition of a lot of NaOH solution was that pancreatic lipases were easily accessible to the oil-in-water interface (Cheong et al., 2016). The amounts of FFAs released at the 120 min were ranged from 89% to 97%. These results indicated that FFAs were being generated in these samples in consequence of the conversion of triacylglycerols into two free fatty acids and monoacylglycerols by the action of lipase (Qian et al., 2012a). The final extent of lipid digestion calculated after small intestinal phase was fairly similar in both samples before and after freeze-drying. The rate of digestion of 96GS-FH was not also

statistically significant, however, it was noticeably slow when referring to the results presented in the graph (Fig. 13a). This result was due to the smaller molecular weight of 96GS, which made it difficult for the lipase in the aqueous phase to easily disperse through the hydrogel and access the surface of the encapsulated lipids and as the 96GS was more tightly covered around the oil in the form of filled hydrogel (McClements David JulianandLi, 2010). The transit time in gastrointestinal tract was increased by the slower rate of lipid digestion, which could prolong the period of release and absorption of bioactive substances in small intestine (Cheong et al., 2016; McClements David Julian et al., 2015). Meanwhile, it was assumed that the rate and extent of lipid digestion among the samples were not significantly different, since 4% of oil contained in all samples was small enough not to affect the results. It is necessary to measure the lipid digestion of curcumin by increasing the ratio of oils contained in emulsion and filled hydrogels in future studies.

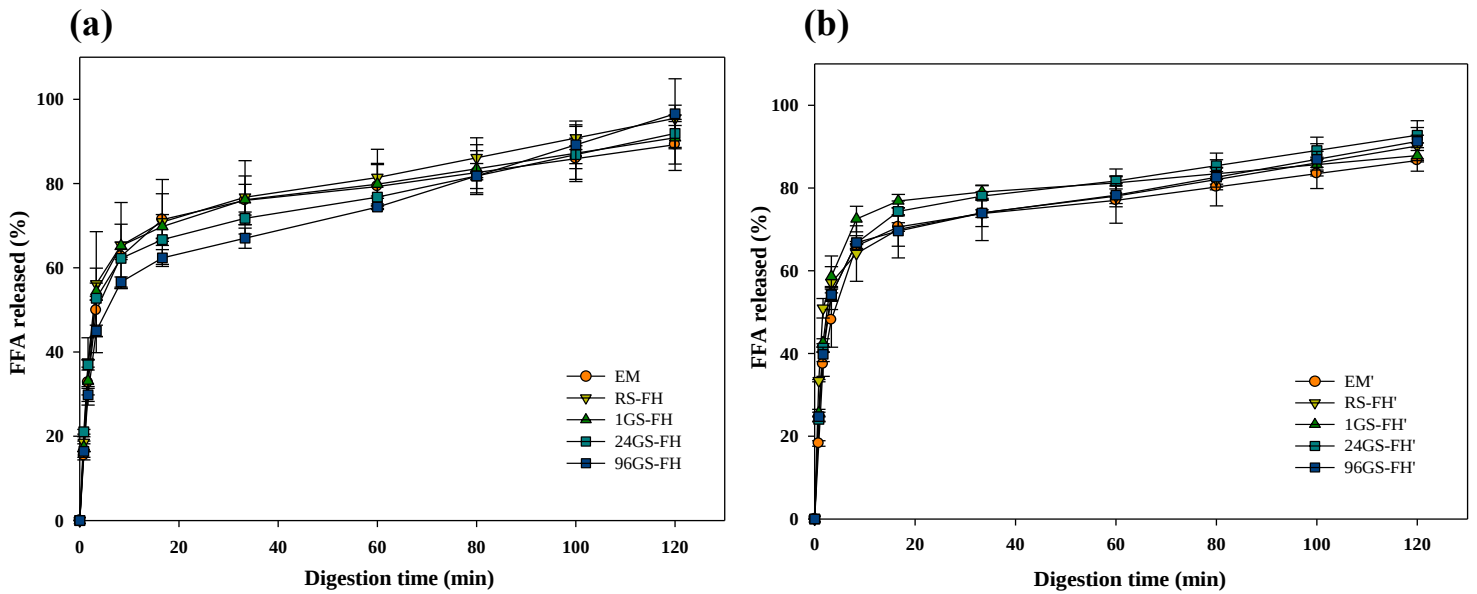


**Fig. 12. Release profiles of free fatty acid (FFA) released from (a) EM, RS-FH, 1GS-FH, 24GS-FH, and 96GS-FH (b) EM', RS-FH', 1GS-FH', 24GS-FH', and 96GS-FH'**

### 5.2.4.2. Confocal laser scanning microscopy (CLSM)

The microstructural changes of the curcumin encapsulation systems were measured using the confocal laser scanning microscopy to interpret the rate of lipid digestion and curcumin retention (Fig. 13A and B). The lipid droplet size of EM increased and some coalescence of the lipid droplets were produced in the oral and gastric phases, and the confocal image disappeared in the small intestine phase due to lipid droplet digestion by lipase (Fig. 13Aa). Flocculation and coalescence are two of the several factors that cause emulsion instability. Flocculation of lipid droplet tends to occur when the attractive interactions (e.g. van der Waals, hydrophobic, and deletion) acting between the droplets overweigh the repulsive interactions (e.g. steric and electrostatic) (McClements David Julian, 2015). The particles maintain their structural integrity during flocculation (McClements D JulianandDemetriades, 1998). Meanwhile, coalescence happens when two colliding droplets will form a single larger droplet (Rousseau, 2000). This phenomenon tends to occur when the attractive forces acting between the droplets outweigh the repulsive forces (similar to flocculation), and the interfacial layers around the oil droplets rupture when the droplets come into contact (Adams et al., 2007; Tcholakova et al., 2006). Therefore, some coalescence and flocculation of ingested lipid droplets in the oral and gastric phases may be

attributed to the depletion flocculation and bridging mechanism caused by non-accreted mucin in the simulated saliva (McClements David JulianandLi, 2010; Vingerhoeds et al., 2005; Zhang Zipei et al., 2016). These mucin molecules produced an osmotic attraction between the lipid droplets that allowed them together, resulting in a change in particle size (Zhang Zipei et al., 2016).

Meanwhile, FH samples (RS-FH, 1GS-FH, 24GS-FH, and 96GS-FH) indicated some flocculation of the lipid droplets in the oral phase, but showed differences in microstructures in the gastric phase depending on the hydrogel types (Fig. 13A b-e). The fine lipid droplets of RS-FH showed both coalescence and flocculation at the oral phase, but were dispersed quite uniformly throughout. However, the large coalescence of lipid droplets was observed when exposed to gastric juice (Fig. 13Ab). As can be seen in Fig 13A c-e, GS-FH showed only slight coalescence not only in the gastric phase as well as in the oral phase, suggesting that the lipid droplets were still trapped in the hydrogel network. As mentioned above (section 4.1.2.4.3.), GS has weaker gel strength than RS, but could form a compactly packed gel network with a relatively reduced molecular weight and narrow molecular weight distribution. In addition, there is the difference between the gel network structure of RS-FH and GS-FH as shown in Fig. 1B. RS-FH forms a distinct three-dimensional network structure, while GS-

FH makes a weak gel in condition in which GS molecules are evenly distributed around the oil due to quite lower molecular weight of GS. Therefore, GS may have filled the emulsion oil more densely to slow the diffusion of reactants, catalysts, and products involved in the lipolysis process. Previous study reported that the starch-based hydrogel prevented the aggregation of the oil droplets by forming a highly viscous aqueous phase that delayed droplet movement (Mun et al., 2016). The results also showed that partial hydrolysis of the starch gel network by the action of α-amylase in the oral phase affected the oil protective effect in samples. In addition, the starch particles prevented the hydrolysis of WPI from by pepsin in the gastric phase, so that a large size of lipid droplets by coalescence were less observed than the emulsion system. It was confirmed that the unique gelation properties of GS acted as an important factor influencing the stability of the oil in this study. Meanwhile, the sizes of coalesced lipid droplets of EMP' in the oral and gastric phases were greater than that of EM. In addition, lipid droplets of FH' samples in the oral phase represented considerably more coalescence than FH samples (Fig. 13A b-e, 13B g-j), and those in the gastric phase also indicated larger sizes and greater coalescence than FH samples. This results were due to the destabilization of emulsion caused by freeze-drying process, which promoted the collapse of the interfacial layers around the oil droplets (Tcholakova et al., 2006)

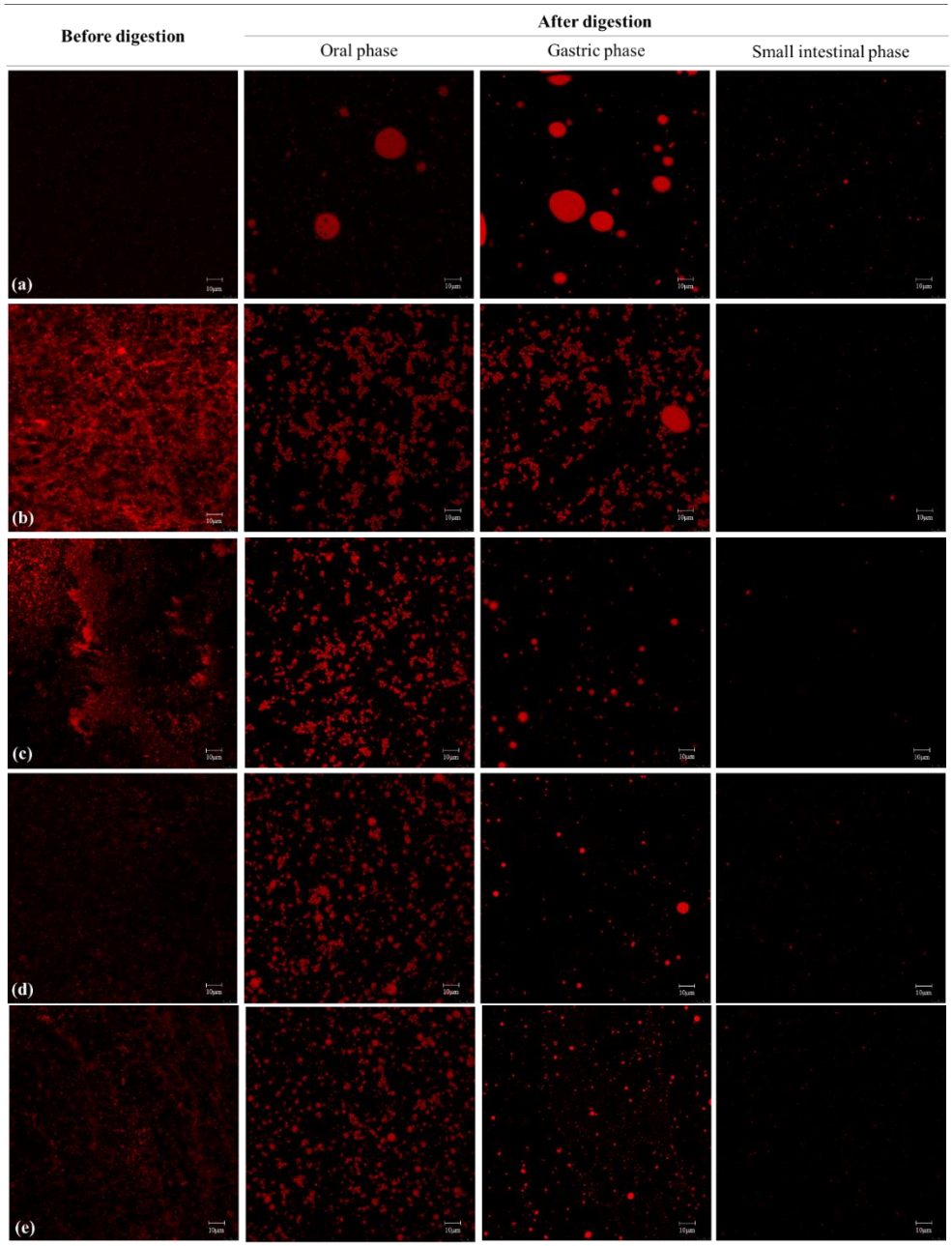


**Fig. 13. (A) Microstructural changes in (a) EM, (b) RS-FH, (c) 1GS-FH, (d) 24GS-FH and (e) 96GS-FH determined using CLSM during *in vitro* digestion. Scale bar is 10 µm.**

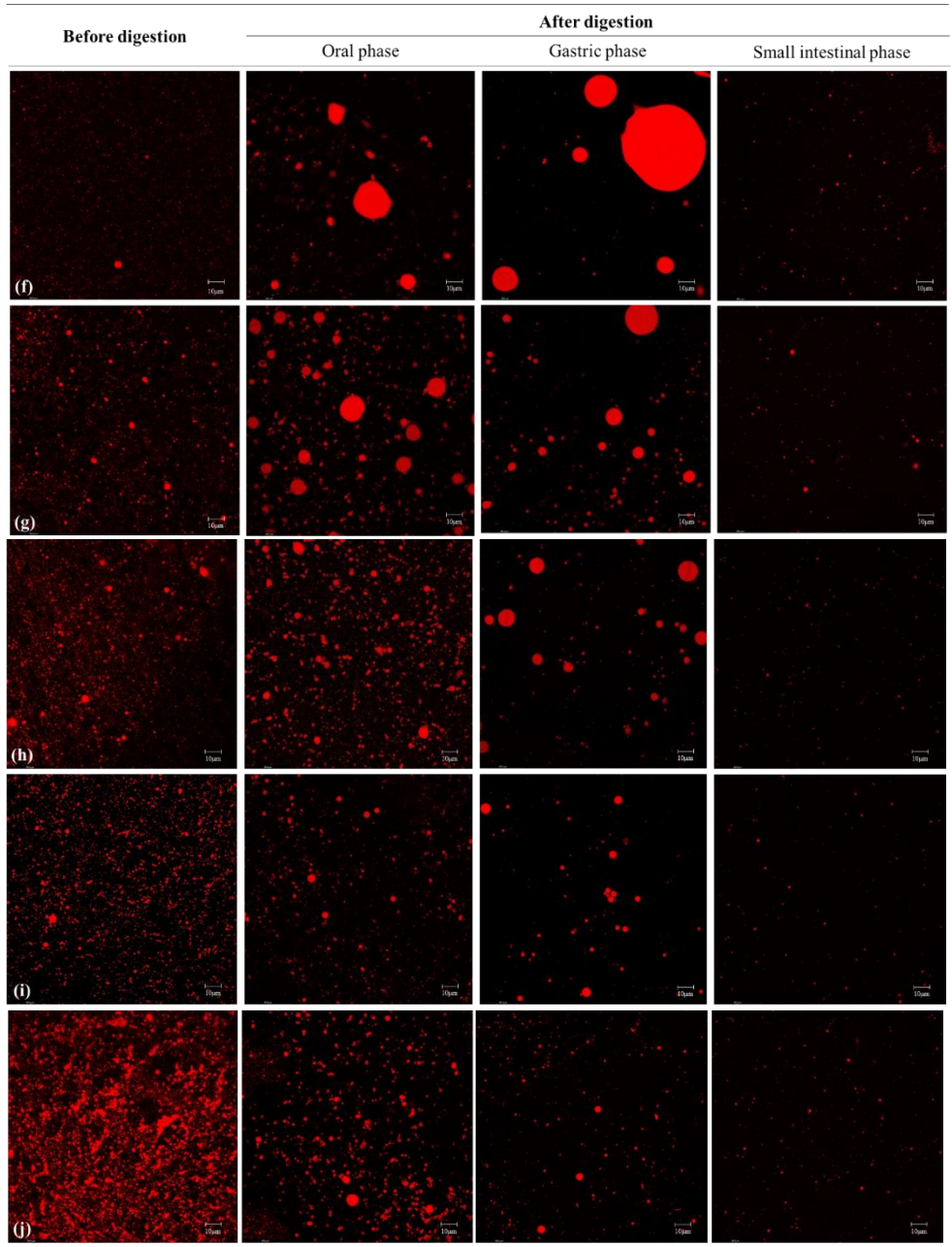


**Fig. 13. (B) Microstructural changes in (f) EM', (g) RS-FH', (h) 1GS-FH', (i) 24GS-FH' and (j) 96GS-FH' determined using CLSM during *in vitro* digestion. Scale bar is 10 µm.**

### 5.2.4.3. Curcumin retention rate

The influence of the presence or absence of the starch particles in emulsion on curcumin retention under simulated physiological environmental conditions consisted of oral, stomach, and intestinal phases was measured (Fig. 14a and b). The curcumin retention (%) refers to the amount of compound that actually remains in the food matrix while passing through the GIT tract. Normally, bioaccessibility can be obtained through *in vitro* digestion system and it occasionally needs a filtering process to calculate the exact value (to mimic the intestinal pore size) (Park S. et al., 2018; Qian et al., 2012a). However, in this study the curcumin retention (%) was measured due to the inaccuracy in the filtering process for estimating bioaccessibility (as shown in Fig. 14a and b). Curcumin retention (%) means the value of raw digesta divided by the initial amount of curcumin.

During gastrointestinal digestion, a synergistic interaction between enzyme and pH conditions resulted in significant breakdown of Cur (retention rate: approx. 34.7%). The degradation of the curcumin is believed to be caused by partial deprotonation in the aqueous solution, which is expected to produce substances in vanillin, ferulic and ferulic acid methane (Liu F. et al., 2018). Such a reaction is known to be caused by direct contact with aqueous phase, it is thought that

enzymatically treated starch particles protect the surface of curcumin and block contact with water to improve stability of curcumin. It also shown that the curcumin encapsulation system clearly had a significant effect on curcumin retention after the digestive process ($p < 0.05$). Generally, in the absence of lipid digestion products, because the bile salts and phospholipids in the intestinal fluids only form simple mixed micelles in the intestinal fluid, and thus the absorption rate of the hydrophobic bioactive compounds after digestion is relatively low (Ahmed K. et al., 2012; Porter et al., 2004). Since the curcumin encapsulation systems prepared in our study contained lipids to form mixed micelles in the intestine, a significant comparison of curcumin retention was possible. As can be seen in Fig. 16a, it was confirmed that the EM and RS-FH system retained at least 50.1% and 68.1% of the encapsulated curcumin, respectively, after digestion, showing a slower and more efficient release than the control (free curcumin). EM may be attributed to the increased formation of mixed micelles in which curcumin can be dissolved and transported under simulated small intestinal conditions as in the previous study (Porter et al., 2008). Both the 1GS-FH (approx. 80.2%) and 96GS-FH (approx. 90.1%) system showed significant curcumin protection, due to the effect of hydrogel to prevent droplet aggregation in the GIT as shown in previous studies by confocal laser microscopy (Mun et al., 2015; Mun et al., 2016). In particular, the droplets of 96GS-FH were more effectively

wrapped by a polymer made up of small molecular weights, it could increase the stability of the emulsion and prevent the decomposition of curcumin within the digestive model system especially in the stomach phase of strong acidity. Based on these results, it can be expected that 96GS-FH prevented curcumin degradation by protecting the emulsion under the strong acidic condition and inhibiting the action of pepsin to degrades emulsifier (WPI) in stomach phase by the reversible aggregation characteristic of 96GS. Meanwhile, samples rehydrated after the freeze drying (EM', RS-FH', 1GS-FH', 24GS-FH', and 96GS-FH') were similar in tendency compared to the original EM and FH samples, but their curcumin retention values were all reduced (Fig. 14a and b). As mentioned in sec. 5.2.4.2 earlier, it was assumed that emulsion instability in the process of freezing drying resulted from less protection of oil from environment with pH-variation and enzyme reaction during the digestive system process.

RS and GS used in FH differed significantly in molecular weight distribution and gelation properties (sec. 5.1.1. and 5.1.3.). Based on those results, GS showed a higher curcumin protective effect than RS, but more precise molecular mechanisms need further research. The FH system maintained the semi-solid structure even after exposure to the digestion stage by the gel network, thereby

increasing the stability of curcumin and the formation of mixed micelles was well achieved. It is thought that this high level of retention due to the formation of high mixed micelles will significantly increase the bioaccessibility of curcumin.

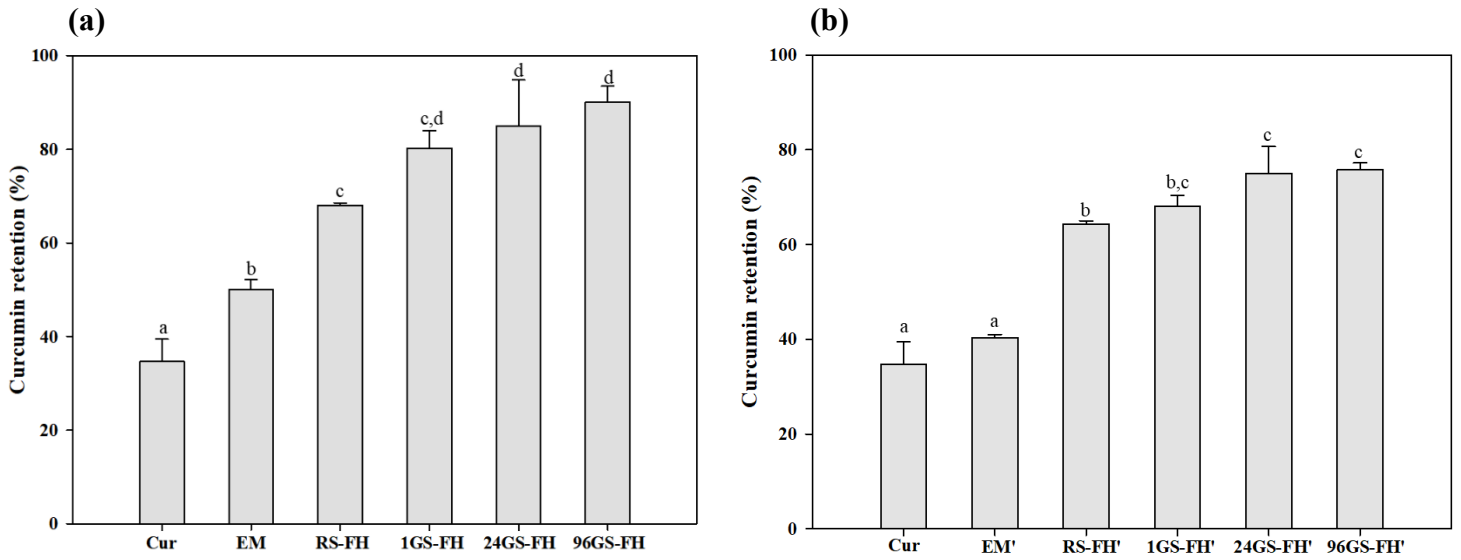


**Fig. 14. Retention rate of (a) curcumin (Cur), EM, RS-FH, 1GS-FH, 24GS-FH, and 96GS-FH (EM and FH before freeze-drying) (b) Cur, EM', RS-FH', 1GS-FH', 24GS-FH', and 96GS-FH' (EM and FH after freeze-drying)**

#### 5.2.4.4. Caco-2 cell cytotoxicity

Cell viability was determined using the MTT assay to evaluate the cytotoxicity of digesta samples on Caco-2 cells. MTT is a yellow tetrazolium salt that is oxidized by the mitochondrial dehydrogenase in living cells to provide a dark blue formazan (Wahlang et al., 2011). Cell viability value of less than 50% shows diminished mitochondrial activity (Li M. et al., 2015). The concentration of samples to be loaded is considered to be non-toxic to the cells when the cell viability is 80% or more (Wahlang et al., 2011). As shown in Fig. 15, cell viability increased as the samples were diluted. When all samples were diluted 16 times, the cell viability was found to be well over 80%. However, the cell viability of samples diluted 8 times also exceeded 80% except RS-FH, and that of RS-FH was about 75.19%, nearly close to 80%. Therefore, the proposed samples concentration was determined as 12-fold dilution rate, which was between 8- and 16- dilution rate.

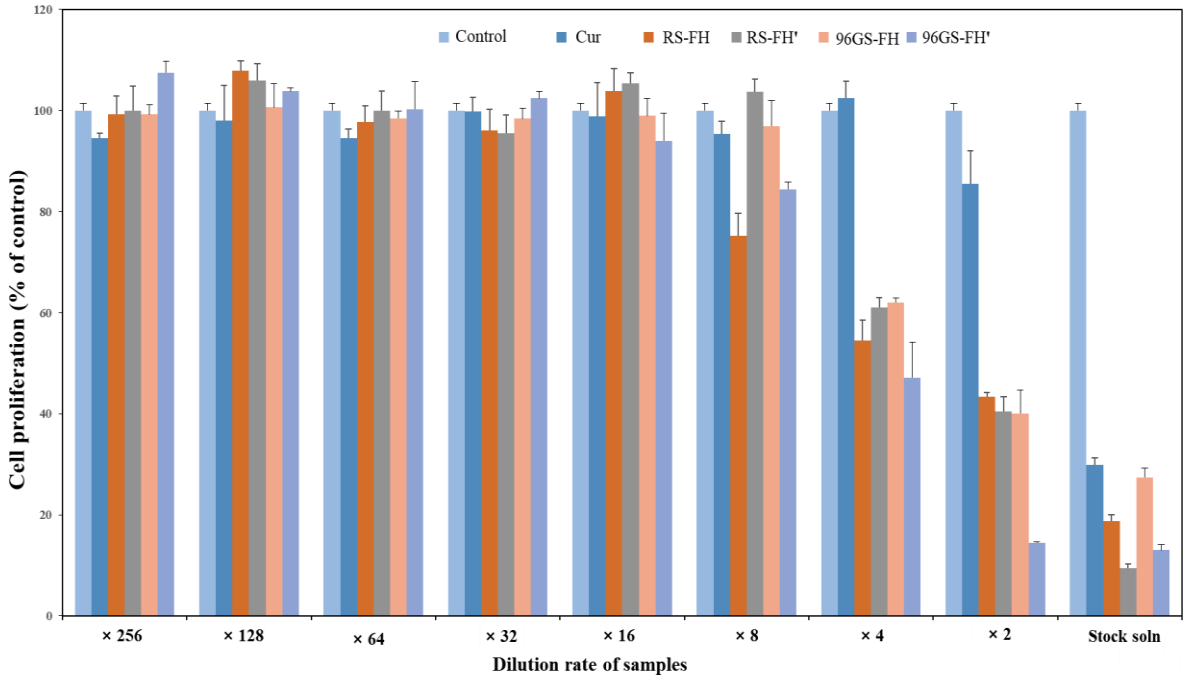


**Fig. 15. Cytotoxicity results of samples (Cur, RS-FH, RS-FH', 96GS-FH, and 96GS-FH') at different dilution rate in Caco-2 cells using the MTT assay.**

### 5.2.4.5. Curcumin bioavailability

As shown in Fig. 16, the bioavailability of Cur was about 1.50±0.35% after 2h incubation. Among FH and FH' samples, RS-FH had a bioavailability of approximately 1.73±0.39%, but the bioavailability of remaining samples was not detected.

Previous studied reported that curcumin encapsulated in nanoemulsions, nanosuspensions using β-lactoglobulin, or nanofibers could be enhanced its bioavailability, which was attribute to the effect of increasing solubility of encapsulated curcumin or the function of added polymers (AdityaandYangand et al., 2015; Faralli et al., 2019; Li M. et al., 2015). In the studies mentioned in the reference, the concentration of curcumin loaded for permeability was about 55 to 100 ppm. However, the concentration of samples taken in this study averaged 0.16 to 0.83 ppm. The reason why the concentration of samples was extremely low was not only because the concentration of oil containing curcumin in emulsion was low (4%), but because the experiment was conducted by diluting it 12 times after going through the *in vitro* model system. Therefore, the samples used in this study were not suitable for accurate bioavailability measurements.

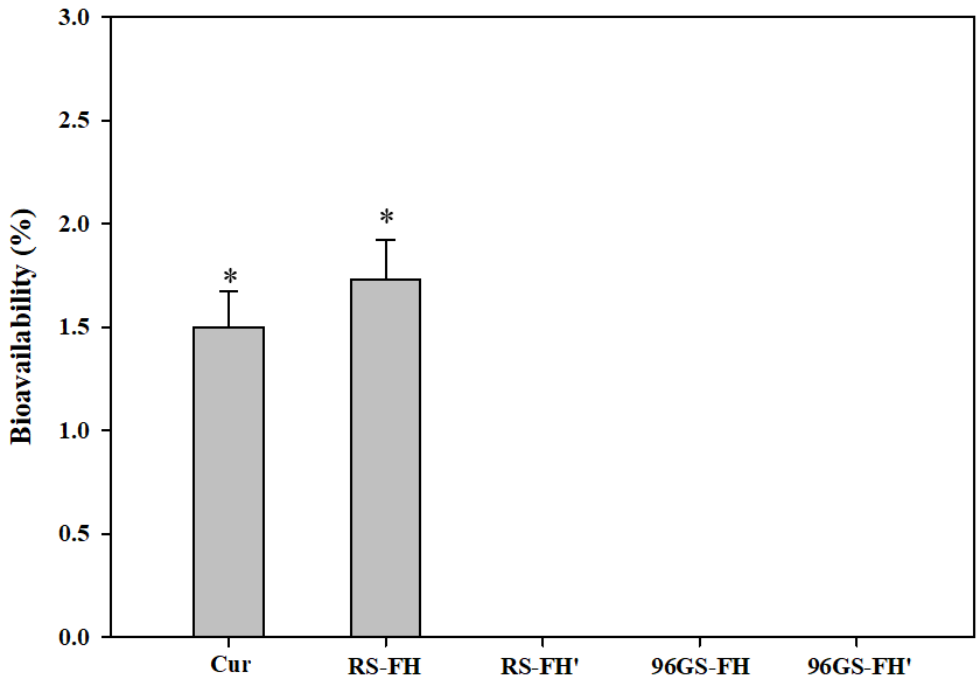


**Fig. 16. *In vitro* bioavailability of samples (Cur, RS-FH, RS-FH', 96GS-FH, and 96GS-FH')**

## 6. Conclusions

In this study, it was confirmed that 4αGTase-treated rice starch-based filled hydrogel (GS-FH) significantly improved the encapsulation efficiency of curcumin in emulsions ($p < 0.05$). The study showed that the UV stability of curcumin with FH was improved by up to 2.28-fold compared to that of emulsion system. However, GS-FH did not show the effects of curcumin protection in heat stability than EM. Meanwhile, 1GS- (80.2%), 24GS- (85.0%), and 96GS-FH (90.1%) improved stability and curcumin retention rate after *in vitro* digestion system compared to free curcumin (34.7%), emulsion (50.1%), RS-FH (68.1%) samples. The improved curcumin retention with GS may be attributed to the overall increase in the number of long branched chains and a decrease in molecular weight, which exhibited more effectively covered around the oil in the form of FH. Therefore, GS could successfully protect curcumin dissolved in the lipid phase of the emulsion by hydrogel form under the environments with pH-variation. The results of this study confirmed the applicability of the GS hydrogel as food-grade bioactive delivery system to improve the chemical stability of curcumin.

# 7. References


Abbas, K., Khalil, S. K., & Hussin, A. S. M. (2010). Modified starches and their usages in selected food products: a review study. *Journal of Agricultural Science, 2*(2), 90.

Adams, F., Walstra, P., Brooks, B., Richmond, H., Zerfa, M., Bibette, J., . . . Kabalnov, A. (2007). *Modern aspects of emulsion science*: Royal Society of Chemistry.

Aditya, N., Aditya, S., Yang, H., Kim, H. W., Park, S. O., & Ko, S. (2015). Co-delivery of hydrophobic curcumin and hydrophilic catechin by a water-in-oil-in-water double emulsion. *Food Chemistry, 173*, 7-13.

Aditya, N., Yang, H., Kim, S., & Ko, S. (2015). Fabrication of amorphous curcumin nanosuspensions using β-lactoglobulin to enhance solubility, stability, and bioavailability. *Colloids and Surfaces B: Biointerfaces, 127*, 114-121.

Ahmed, E. M. (2015). Hydrogel: Preparation, characterization, and applications: A review. *Journal of advanced research, 6*(2), 105-121.

Ahmed, K., Li, Y., McClements, D. J., & Xiao, H. (2012). Nanoemulsion-and emulsion-based delivery systems for curcumin: encapsulation and release properties. *Food Chemistry, 132*(2), 799-807.

Akhtar, M. F., Hanif, M., & Ranjha, N. M. (2016). Methods of synthesis of hydrogels… A review. *Saudi Pharmaceutical Journal, 24*(5), 554-559.

Akram, M., Shahab-Uddin, A. A., Usmanghani, K., Hannan, A., Mohiuddin, E., & Asif, M. (2010). Curcuma longa and curcumin: a review article. *Rom J Biol Plant Biol, 55*(2), 65-70.

Ali, B. H., Marrif, H., Noureldayem, S. A., Bakheit, A. O., & Blunden, G. (2006).

Some biological properties of curcumin: A review. *Natural Product Communications, 1*(6), 1934578X0600100613.

Amagliani, L., O'Regan, J., Kelly, A. L., & O'Mahony, J. A. (2016). Chemistry, structure, functionality and applications of rice starch. *Journal of Cereal Science, 70*, 291-300.

Anwar, S. H., & Kunz, B. (2011). The influence of drying methods on the stabilization of fish oil microcapsules: Comparison of spray granulation, spray drying, and freeze drying. *Journal of Food Engineering, 105*(2), 367-378.

Bates, F. L., French, D., & Rundle, R. (1943). Amylose and amylopectin content of starches determined by their iodine complex formation1. *Journal of the American Chemical Society, 65*(2), 142-148.

Bhushani, J. A., Karthik, P., & Anandharamakrishnan, C. (2016). Nanoemulsion based delivery system for improved bioaccessibility and Caco-2 cell monolayer permeability of green tea catechins. *Food Hydrocolloids, 56*, 372-382.

Biduski, B., da Silva, W. M. F., Colussi, R., El Halal, S. L. d. M., Lim, L.-T., Dias, Á. R. G., & da Rosa Zavareze, E. (2018). Starch hydrogels: The influence of the amylose content and gelatinization method. *International journal of biological macromolecules, 113*, 443-449.

Biliaderis, C. G. (2009). Structural transitions and related physical properties of starch. In *Starch* (pp. 293-372): Elsevier.

Calero, N., Muñoz, J., Cox, P. W., Heuer, A., & Guerrero, A. (2013). Influence of chitosan concentration on the stability, microstructure and rheological properties of O/W emulsions formulated with high-oleic sunflower oil and potato protein. *Food Hydrocolloids, 30*(1), 152-162.

Cano-Higuita, D., Malacrida, C., & Telis, V. (2015). Stability of curcumin microencapsulated by spray and freeze drying in binary and ternary matrices of maltodextrin, gum arabic and modified starch. *Journal of food processing and preservation, 39*(6), 2049-2060.

Che, L.-M., Wang, L.-J., Li, D., Bhandari, B., Özkan, N., Chen, X. D., & Mao, Z.-H. (2009). Starch pastes thinning during high-pressure homogenization. *Carbohydrate polymers, 75*(1), 32-38.

Cheetham, N. W., & Tao, L. (1998). Variation in crystalline type with amylose content in maize starch granules: an X-ray powder diffraction study. *Carbohydrate Polymers, 36*(4), 277-284.

Chen, B., Zhang, B., Li, M.-N., Xie, Y., & Chen, H.-Q. (2018). Effects of glutenin and gliadin modified by protein-glutaminase on pasting, rheological properties and microstructure of potato starch. *Food Chemistry, 253*, 148-155.

Cheong, A. M., Tan, C. P., & Nyam, K. L. (2016). In vitro evaluation of the structural and bioaccessibility of kenaf seed oil nanoemulsions stabilised by binary emulsifiers and β-cyclodextrin complexes. *Journal of food engineering, 189*, 90-98.

Cho, K.-H., Auh, J.-H., Ryu, J.-H., Kim, J.-H., Park, K., Park, C.-S., & Yoo, S.-H. (2009). Structural modification and characterization of rice starch treated by Thermus aquaticus 4-α-glucanotransferase. *Food Hydrocolloids, 23*(8), 2403-2409.

Colombo, P. (1993). Swelling-controlled release in hydrogel matrices for oral route. *Advanced Drug Delivery Reviews, 11*(1-2), 37-57.

Dai, L., Li, R., Wei, Y., Sun, C., Mao, L., & Gao, Y. (2018). Fabrication of zein and rhamnolipid complex nanoparticles to enhance the stability and in

vitro release of curcumin. *Food Hydrocolloids, 77*, 617-628.

Das, N. (2013). Preparation methods and properties of hydrogel: a review. *Int J Pharm Pharm Sci, 5*(3), 112-117.

Dhital, S., Butardo Jr, V. M., Jobling, S. A., & Gidley, M. J. (2015). Rice starch granule amylolysis–Differentiating effects of particle size, morphology, thermal properties and crystalline polymorph. *Carbohydrate Polymers, 115*, 305-316.

Dickinson, E. (2003). Hydrocolloids at interfaces and the influence on the properties of dispersed systems. *Food Hydrocolloids, 17*(1), 25-39.

Dickinson, E. (2009). Hydrocolloids as emulsifiers and emulsion stabilizers. *Food Hydrocolloids, 23*(6), 1473-1482.

Do, H. V., Lee, E.-J., Park, J.-H., Park, K.-H., Shim, J.-Y., Mun, S., & Kim, Y.-R. (2012). Structural and physicochemical properties of starch gels prepared from partially modified starches using Thermus aquaticus 4-α-glucanotransferase. *Carbohydrate Polymers, 87*(4), 2455-2463.

Esatbeyoglu, T., Huebbe, P., Ernst, I. M., Chin, D., Wagner, A. E., & Rimbach, G. (2012). Curcumin—from molecule to biological function. *Angewandte Chemie International Edition, 51*(22), 5308-5332.

Faralli, A., Shekarforoush, E., Ajalloueian, F., Mendes, A. C., & Chronakis, I. S. (2019). In vitro permeability enhancement of curcumin across Caco-2 cells monolayers using electrospun xanthan-chitosan nanofibers. *Carbohydrate Polymers, 206*, 38-47.

Fennema, E., & Peterson, P. (1985). Autonomous learning behavior: A possible explanation of gender-related differences in mathematics. In *Gender influences in classroom interaction* (pp. 17-35): Elsevier.

Fioramonti, S. A., Rubiolo, A. C., & Santiago, L. G. (2017). Characterisation of

freeze-dried flaxseed oil microcapsules obtained by multilayer emulsions. *Powder technology, 319*, 238-244.

Ghaleshahi, A. Z., & Rajabzadeh, G. (2020). The influence of sodium alginate and genipin on physico-chemical properties and stability of WPI coated liposomes. *Food Research International, 130*, 108966.

Glaze, W. H., Lay, Y., & Kang, J.-W. (1995). Advanced oxidation processes. A kinetic model for the oxidation of 1, 2-dibromo-3-chloropropane in water by the combination of hydrogen peroxide and UV radiation. *Industrial & Engineering Chemistry Research, 34*(7), 2314-2323.

Goel, A., Kunnumakkara, A. B., & Aggarwal, B. B. (2008). Curcumin as "Curecumin": from kitchen to clinic. *Biochemical pharmacology, 75*(4), 787-809.

Gulrez, S. K., Al-Assaf, S., & Phillips, G. O. (2011). Hydrogels: methods of preparation, characterisation and applications. *Progress in molecular and environmental bioengineering—from analysis and modeling to technology applications*, 117-150.

Guraya, H. S., James, C., & Champagne, E. T. (2001). Effect of enzyme concentration and storage temperature on the formation of slowly digestible starch from cooked debranched rice starch. *Starch-Stärke, 53*(3-4), 131-139.

Hasan, M., Belhaj, N., Benachour, H., Barberi-Heyob, M., Kahn, C., Jabbari, E., . . . Arab-Tehrany, E. (2014). Liposome encapsulation of curcumin: physico-chemical characterizations and effects on MCF7 cancer cell proliferation. *International journal of pharmaceutics, 461*(1-2), 519-528.

Heger, M., van Golen, R. F., Broekgaarden, M., & Michel, M. C. (2014). The molecular basis for the pharmacokinetics and pharmacodynamics of

curcumin and its metabolites in relation to cancer. *Pharmacological reviews, 66*(1), 222-307.

Immel, S., & Lichtenthaler, F. W. (2000). The hydrophobic topographies of amylose and its blue iodine complex. *Starch-Stärke, 52*(1), 1-8.

Jenkins, P., & Donald, A. (1995). The influence of amylose on starch granule structure. *International journal of biological macromolecules, 17*(6), 315-321.

Jiang, H., Miao, M., Ye, F., Jiang, B., & Zhang, T. (2014). Enzymatic modification of corn starch with 4-α-glucanotransferase results in increasing slow digestible and resistant starch. *International journal of biological macromolecules, 65*, 208-214.

Jin, H.-R., Yu, J., & Choi, S.-J. (2020). Hydrothermal Treatment Enhances Antioxidant Activity and Intestinal Absorption of Rutin in Tartary Buckwheat Flour Extracts. *Foods, 9*(1), 8.

Joung, H. J., Choi, M. J., Kim, J. T., Park, S. H., Park, H. J., & Shin, G. H. (2016). Development of food-grade curcumin nanoemulsion and its potential application to food beverage system: antioxidant property and in vitro digestion. *Journal of food science, 81*(3), N745-N753.

Jung, W.-J., Han, J.-A., & Lim, S.-T. (2010). Thermal and rheological properties of hydrogels prepared with retrograded waxy rice starch powders. *Food Science and Biotechnology, 19*(6), 1649-1654.

Kaper, T., Van der Maarel, M., Euverink, G., & Dijkhuizen, L. (2004). Exploring and exploiting starch-modifying amylomaltases from thermophiles. Portland Press Ltd.

Kasprzak, M. M., Macnaughtan, W., Harding, S., Wilde, P., & Wolf, B. (2018). Stabilisation of oil-in-water emulsions with non-chemical modified

gelatinised starch. *Food Hydrocolloids, 81*, 409-418.

Kaur, K., & Singh, N. (2000). Amylose-lipid complex formation during cooking of rice flour. *Food Chemistry, 71*(4), 511-517.

Kaushik, V., & Roos, Y. H. (2007). Limonene encapsulation in freeze-drying of gum Arabic–sucrose–gelatin systems. *LWT-Food science and technology, 40*(8), 1381-1391.

Keeratiburana, T., Hansen, A. R., Soontaranon, S., Blennow, A., & Tongta, S. (2020). Porous high amylose rice starch modified by amyloglucosidase and maltogenic α-amylase. *Carbohydrate Polymers, 230*, 115611.

Khatoon, S., Sreerama, Y., Raghavendra, D., Bhattacharya, S., & Bhat, K. (2009). Properties of enzyme modified corn, rice and tapioca starches. *Food research international, 42*(10), 1426-1433.

Kim, J. M., Song, J. Y., & Shin, M. (2010). Physicochemical properties of high amylose rice starches purified from Korean cultivars. *Starch-Stärke, 62*(5), 262-268.

Kim, Y.-L., Mun, S., Rho, S.-J., Do, H. V., & Kim, Y.-R. (2017). Influence of physicochemical properties of enzymatically modified starch gel on the encapsulation efficiency of W/O/W emulsion containing NaCl. *Food and bioprocess technology, 10*(1), 77-88.

Kim, Y., Kim, Y.-L., Trinh, K. S., Kim, Y.-R., & Moon, T. W. (2012). Texture properties of rice cakes made of rice flours treated with 4-α-glucanotransferase and their relationship with structural characteristics. *Food Science and Biotechnology, 21*(6), 1707-1714.

Kim, Y., Yoo, S.-H., Park, K.-H., Shim, J.-H., & Lee, S. (2012). Functional characterization of native starches through thermal and rheological analysis. *Journal of the Korean Society for Applied Biological Chemistry,*

*55*(3), 413-416.

Knuston, A., & Tao, T. (1999). The honeycomb model of GLn (C) tensor products I: Proof of the saturation conjecture. *J. Amer. Math. Soc, 12*, 1055-1090.

Kong, X., Zhu, P., Sui, Z., & Bao, J. (2015). Physicochemical properties of starches from diverse rice cultivars varying in apparent amylose content and gelatinisation temperature combinations. *Food Chemistry, 172*, 433-440.

Kossmann, J., & Lloyd, J. (2000). Understanding and influencing starch biochemistry. *Critical Reviews in Plant Sciences, 19*(3), 171-226.

Kuriki, T., & Imanaka, T. (1999). The concept of the α-amylase family: structural similarity and common catalytic mechanism. *Journal of bioscience and bioengineering, 87*(5), 557-565.

Le Corre, D., Bras, J., & Dufresne, A. (2010). Starch nanoparticles: a review. *Biomacromolecules, 11*(5), 1139-1153.

Lee, B. H., Choi, H. A., Kim, M.-R., & Hong, J. (2013). Changes in chemical stability and bioactivities of curcumin by ultraviolet radiation. *Food Science and Biotechnology, 22*(1), 279-282.

Lee, K. Y., Kim, Y.-R., Park, K. H., & Lee, H. G. (2006). Effects of α-glucanotransferase treatment on the thermo-reversibility and freeze-thaw stability of a rice starch gel. *Carbohydrate polymers, 63*(3), 347-354.

Lee, K. Y., Kim, Y.-R., Park, K. H., & Lee, H. G. (2008). Rheological and gelation properties of rice starch modified with 4-α-glucanotransferase. *International journal of biological macromolecules, 42*(3), 298-304.

Lee, S. H., Choi, S. J., Shin, S. I., Park, K. H., & Moon, T. W. (2008). Structural and rheological properties of sweet potato starch modified with 4-α-glucanotransferase from Thermus aquaticus. *Food Science and*

*Biotechnology, 17*(4), 705-712.

Li, J., Hwang, I.-C., Chen, X., & Park, H. J. (2016). Effects of chitosan coating on curcumin loaded nano-emulsion: Study on stability and in vitro digestibility. *Food Hydrocolloids, 60*, 138-147.

Li, J., Shin, G. H., Lee, I. W., Chen, X., & Park, H. J. (2016). Soluble starch formulated nanocomposite increases water solubility and stability of curcumin. *Food Hydrocolloids, 56*, 41-49.

Li, M., Cui, J., Ngadi, M. O., & Ma, Y. (2015). Absorption mechanism of whey-protein-delivered curcumin using Caco-2 cell monolayers. *Food Chemistry, 180*, 48-54.

Li, M., Ma, Y., & Cui, J. (2014). Whey-protein-stabilized nanoemulsions as a potential delivery system for water-insoluble curcumin. *LWT-Food science and technology, 59*(1), 49-58.

Li, Y., Li, C., Gu, Z., Hong, Y., Cheng, L., & Li, Z. (2017). Effect of modification with 1, 4-α-glucan branching enzyme on the rheological properties of cassava starch. *International journal of biological macromolecules, 103*, 630-639.

Li, Z.-l., Peng, S.-f., Chen, X., Zhu, Y.-q., Zou, L.-q., Liu, W., & Liu, C.-m. (2018). Pluronics modified liposomes for curcumin encapsulation: Sustained release, stability and bioaccessibility. *Food Research International, 108*, 246-253.

LIEBL, W., FEIL, R., GABELSBERGER, J., KELLERMANN, J., & SCHLEIFER, K. H. (1992). Purification and characterization of a novel thermostable 4-α-glucanotransferase of Thermotoga maritima cloned in Escherichia coli. *European Journal of Biochemistry, 207*(1), 81-88.

Lii, C.-Y., Tsai, M.-L., & Tseng, K.-H. (1996). Effect of amylose content on the

rheological property of rice starch. *Cereal chemistry, 73*(4), 415-420.

Lima-Tenório, M. K., Tenório-Neto, E. T., Guilherme, M. R., Garcia, F. P., Nakamura, C. V., Pineda, E. A., & Rubira, A. F. (2015). Water transport properties through starch-based hydrogel nanocomposites responding to both pH and a remote magnetic field. *Chemical Engineering Journal, 259*, 620-629.

Liu, D., Cheng, B., Li, D., Li, J., Wu, Q., & Pan, H. (2018). Investigations on the interactions between curcumin loaded vitamin E TPGS coated nanodiamond and Caco-2 cell monolayer. *International journal of pharmaceutics, 551*(1-2), 177-183.

Liu, F., Ma, D., Luo, X., Zhang, Z., He, L., Gao, Y., & McClements, D. J. (2018). Fabrication and characterization of protein-phenolic conjugate nanoparticles for co-delivery of curcumin and resveratrol. *Food Hydrocolloids, 79*, 450-461.

Mangolim, C. S., Moriwaki, C., Nogueira, A. C., Sato, F., Baesso, M. L., Neto, A. M., & Matioli, G. (2014). Curcumin–β-cyclodextrin inclusion complex: stability, solubility, characterisation by FT-IR, FT-Raman, X-ray diffraction and photoacoustic spectroscopy, and food application. *Food Chemistry, 153*, 361-370.

Matalanis, A., Campanella, O., & Hamaker, B. (2009). Storage retrogradation behavior of sorghum, maize and rice starch pastes related to amylopectin fine structure. *Journal of Cereal Science, 50*(1), 74-81.

McClements, D., Decker, E., & Weiss, J. (2007). Emulsion-based delivery systems for lipophilic bioactive components. *Journal of food science, 72*(8), R109-R124.

McClements, D. J. (2015). *Food emulsions: principles, practices, and techniques*:

CRC press.

McClements, D. J., & Demetriades, K. (1998). An integrated approach to the development of reduced-fat food emulsions. *Critical reviews in food science and nutrition, 38*(6), 511-536.

McClements, D. J., & Li, Y. (2010). Review of in vitro digestion models for rapid screening of emulsion-based systems. *Food & function, 1*(1), 32-59.

McClements, D. J., Zou, L., Zhang, R., Salvia-Trujillo, L., Kumosani, T., & Xiao, H. (2015). Enhancing nutraceutical performance using excipient foods: designing food structures and compositions to increase bioavailability. *Comprehensive Reviews in Food Science and Food Safety, 14*(6), 824-847.

Mitchell, C. R. (2009). Rice starches: production and properties. In *Starch* (pp. 569-578): Elsevier.

Mohammadian, M., Salami, M., Momen, S., Alavi, F., Emam-Djomeh, Z., & Moosavi-Movahedi, A. A. (2019). Enhancing the aqueous solubility of curcumin at acidic condition through the complexation with whey protein nanofibrils. *Food Hydrocolloids, 87*, 902-914.

Mohan, P. K., Sreelakshmi, G., Muraleedharan, C., & Joseph, R. (2012). Water soluble complexes of curcumin with cyclodextrins: Characterization by FT-Raman spectroscopy. *Vibrational Spectroscopy, 62*, 77-84.

Mun, S., Choi, Y., Park, S., Surh, J., & Kim, Y.-R. (2014). Release properties of gel-type W/O/W encapsulation system prepared using enzymatically-modified starch. *Food Chemistry, 157*, 77-83.

Mun, S., Choi, Y., Shim, J.-Y., Park, K.-H., & Kim, Y.-R. (2011). Effects of enzymatically modified starch on the encapsulation efficiency and stability of water-in-oil-in-water emulsions. *Food Chemistry, 128*(2),

266-275.

Mun, S., Kim, Y.-L., Kang, C.-G., Park, K.-H., Shim, J.-Y., & Kim, Y.-R. (2009). Development of reduced-fat mayonnaise using 4αGTase-modified rice starch and xanthan gum. *International journal of biological macromolecules, 44*(5), 400-407.

Mun, S., Kim, Y.-R., & McClements, D. J. (2015). Control of β-carotene bioaccessibility using starch-based filled hydrogels. *Food Chemistry, 173*, 454-461.

Mun, S., Park, S., Kim, Y.-R., & McClements, D. J. (2016). Influence of methylcellulose on attributes of β-carotene fortified starch-based filled hydrogels: Optical, rheological, structural, digestibility, and bioaccessibility properties. *Food research international, 87*, 18-24.

Nakorn, K. N., Tongdang, T., & Sirivongpaisal, P. (2009). Crystallinity and rheological properties of pregelatinized rice starches differing in amylose content. *Starch-Stärke, 61*(2), 101-108.

Nimiya, Y., Wang, W., Du, Z., Sukamtoh, E., Zhu, J., Decker, E., & Zhang, G. (2016). Redox modulation of curcumin stability: Redox active antioxidants increase chemical stability of curcumin. *Molecular nutrition & food research, 60*(3), 487-494.

No, J., Shin, M., & Mun, S. Preparation of functional rice cake by using b-carotene-loaded emulsion powder.

Pan, K., Zhong, Q., & Baek, S. J. (2013). Enhanced dispersibility and bioactivity of curcumin by encapsulation in casein nanocapsules. *Journal of agricultural and food chemistry, 61*(25), 6036-6043.

Park, H. R., Rho, S.-J., & Kim, Y.-R. (2019). Solubility, stability, and bioaccessibility improvement of curcumin encapsulated using 4-α-

glucanotransferase-modified rice starch with reversible pH-induced aggregation property. *Food Hydrocolloids, 95*, 19-32.

Park, J.-H., Kim, H.-J., Kim, Y.-H., Cha, H., Kim, Y.-W., Kim, T.-J., . . . Park, K.-H. (2007). The action mode of Thermus aquaticus YT-1 4-α-glucanotransferase and its chimeric enzymes introduced with starch-binding domain on amylose and amylopectin. *Carbohydrate polymers, 67*(2), 164-173.

Park, S., Mun, S., & Kim, Y.-R. (2018). Effect of xanthan gum on lipid digestion and bioaccessibility of β-carotene-loaded rice starch-based filled hydrogels. *Food research international, 105*, 440-445.

Patel, A., Hu, Y., Tiwari, J. K., & Velikov, K. P. (2010). Synthesis and characterisation of zein–curcumin colloidal particles. *Soft Matter, 6*(24), 6192-6199.

Peppas, N., Slaughter, B., Kanzelberger, M., Matyjaszewski, K., & Möller, M. (2012). 9.20–Hydrogels. *M. Editorsin-Chief: Krzysztof & M. Martin (Eds.), Polymer Science: A Comprehensive Reference*, 385-395.

Pérez, S., & Bertoft, E. (2010). The molecular structures of starch components and their contribution to the architecture of starch granules: A comprehensive review. *Starch-Stärke, 62*(8), 389-420.

Perrone, D., Ardito, F., Giannatempo, G., Dioguardi, M., Troiano, G., Lo Russo, L., . . . Lo Muzio, L. (2015). Biological and therapeutic activities, and anticancer properties of curcumin. *Experimental and therapeutic medicine, 10*(5), 1615-1623.

Porter, C. J., Kaukonen, A. M., Boyd, B. J., Edwards, G. A., & Charman, W. N. (2004). Susceptibility to lipase-mediated digestion reduces the oral bioavailability of danazol after administration as a medium-chain lipid-

based microemulsion formulation. *Pharmaceutical research, 21*(8), 1405-1412.

Porter, C. J., Pouton, C. W., Cuine, J. F., & Charman, W. N. (2008). Enhancing intestinal drug solubilisation using lipid-based delivery systems. *Advanced drug delivery reviews, 60*(6), 673-691.

Prasad, K., Murakami, M.-a., Kaneko, Y., Takada, A., Nakamura, Y., & Kadokawa, J.-i. (2009). Weak gel of chitin with ionic liquid, 1-allyl-3-methylimidazolium bromide. *International journal of biological macromolecules, 45*(3), 221-225.

Pulido-Moran, M., Moreno-Fernandez, J., Ramirez-Tortosa, C., & Ramirez-Tortosa, M. (2016). Curcumin and health. *Molecules, 21*(3), 264.

Qian, C., Decker, E. A., Xiao, H., & McClements, D. J. (2012a). Nanoemulsion delivery systems: Influence of carrier oil on β-carotene bioaccessibility. *Food Chemistry, 135*(3), 1440-1447.

Qian, C., Decker, E. A., Xiao, H., & McClements, D. J. (2012b). Physical and chemical stability of β-carotene-enriched nanoemulsions: Influence of pH, ionic strength, temperature, and emulsifier type. *Food Chemistry, 132*(3), 1221-1229.

Qiu, F., Li, Y., Yang, D., Li, X., & Sun, P. (2011). Biodiesel production from mixed soybean oil and rapeseed oil. *Applied Energy, 88*(6), 2050-2055.

Raigond, P., Ezekiel, R., & Raigond, B. (2015). Resistant starch in food: a review. *Journal of the Science of Food and Agriculture, 95*(10), 1968-1978.

Rao, M. A. (2010). *Rheology of fluid and semisolid foods: principles and applications*: Springer Science & Business Media.

Roughley, P., & Whiting, D. (1973). J. chem. Soc, Perkin Trans. I.

Rousseau, D. (2000). Fat crystals and emulsion stability—a review. *Food*

*Research International, 33*(1), 3-14.

Saibene, D., & Seetharaman, K. (2006). Segmental mobility of polymers in starch granules at low moisture contents. *Carbohydrate Polymers, 64*(4), 539-547.

Sarkar, A., Goh, K. K., Singh, R. P., & Singh, H. (2009). Behaviour of an oil-in-water emulsion stabilized by β-lactoglobulin in an in vitro gastric model. *Food Hydrocolloids, 23*(6), 1563-1569.

Schramm, G. (1994). A Practical Approach to Rheology and Rheometry. Rheology, 291.

Shen, L., & Ji, H.-F. (2007). Theoretical study on physicochemical properties of curcumin. *Spectrochimica Acta Part A: Molecular and Biomolecular Spectroscopy, 67*(3-4), 619-623.

Shih, F., King, J., Daigle, K., An, H. J., & Ali, R. (2007). Physicochemical properties of rice starch modified by hydrothermal treatments. *Cereal chemistry, 84*(5), 527-531.

Shon, K. J., & Yoo, B. (2006). Effect of acetylation on rheological properties of rice starch. *Starch-Stärke, 58*(3-4), 177-185.

Singh, J., Dartois, A., & Kaur, L. (2010). Starch digestibility in food matrix: a review. *Trends in Food Science & Technology, 21*(4), 168-180.

Sousdaleff, M., Baesso, M. L., Neto, A. M., Nogueira, A. C. u., Marcolino, V. A., & Matioli, G. (2013). Microencapsulation by freeze-drying of potassium norbixinate and curcumin with maltodextrin: stability, solubility, and food application. *Journal of agricultural and food chemistry, 61*(4), 955-965.

Stephen, A. M., & Phillips, G. O. (2016). *Food polysaccharides and their applications*: CRC press.

Strater, N., Przylas, I., Saenger, W., Terada, Y., Fuji, K., & Takaha, T. (2002).

Structural basis of the synthesis of large cycloamyloses by amylomaltase. *BIOLOGIA-BRATISLAVA-, 57*(SUP/2), 93-100.

Sun, C., Xu, C., Mao, L., Wang, D., Yang, J., & Gao, Y. (2017). Preparation, characterization and stability of curcumin-loaded zein-shellac composite colloidal particles. *Food Chemistry, 228*, 656-667.

Suresh, D., Gurudutt, K., & Srinivasan, K. (2009). Degradation of bioactive spice compound: curcumin during domestic cooking. *European Food Research and Technology, 228*(5), 807-812.

Takaha, T., Yanase, M., Takata, H., Okada, S., & Smith, S. M. (1996). Potato D-enzyme catalyzes the cyclization of amylose to produce cycloamylose, a novel cyclic glucan. *Journal of Biological Chemistry, 271*(6), 2902-2908.

Takaha, T., Yanase, M., Takata, H., Okada, S., & Smith, S. M. (1998). Cyclic glucans produced by the intramolecular transglycosylation activity of potato D-enzyme on amylopectin. *Biochemical and biophysical research communications, 247*(2), 493-497.

Tako, M., & Hizukuri, S. (2002). Gelatinization mechanism of potato starch. *Carbohydrate polymers, 48*(4), 397-401.

Tapal, A., & Tiku, P. K. (2012). Complexation of curcumin with soy protein isolate and its implications on solubility and stability of curcumin. *Food Chemistry, 130*(4), 960-965.

Tcholakova, S., Denkov, N. D., Ivanov, I. B., & Campbell, B. (2006). Coalescence stability of emulsions containing globular milk proteins. *Advances in Colloid and Interface Science, 123*, 259-293.

Tonnesen, H., & Karlsen, J. (1985). Studies on curcumin and curcuminoids. V. Alkaline degradation of curcumin. *Zeitschrift für Lebensmittel-Untersuchung und-Forschung, 180*(2), 132-134.

Tønnesen, H. H., Karlsen, J., & van Henegouwen, G. B. (1986). Studies on curcumin and curcuminoids VIII. Photochemical stability of curcumin. *Zeitschrift für Lebensmittel-Untersuchung und Forschung, 183*(2), 116-122.

van der Maarel, M. J., & Leemhuis, H. (2013). Starch modification with microbial alpha-glucanotransferase enzymes. *Carbohydrate polymers, 93*(1), 116-121.

Vingerhoeds, M. H., Blijdenstein, T. B., Zoet, F. D., & van Aken, G. A. (2005). Emulsion flocculation induced by saliva and mucin. *Food Hydrocolloids, 19*(5), 915-922.

Wahlang, B., Pawar, Y. B., & Bansal, A. K. (2011). Identification of permeability-related hurdles in oral delivery of curcumin using the Caco-2 cell model. *European Journal of Pharmaceutics and Biopharmaceutics, 77*(2), 275-282.

Wang, L.-L., He, D.-D., Wang, S.-X., Dai, Y.-H., Ju, J.-M., & Zhao, C.-L. (2018). Preparation and evaluation of curcumin-loaded self-assembled micelles. *Drug development and industrial pharmacy, 44*(4), 563-569.

Wang, Y.-J., Pan, M.-H., Cheng, A.-L., Lin, L.-I., Ho, Y.-S., Hsieh, C.-Y., & Lin, J.-K. (1997). Stability of curcumin in buffer solutions and characterization of its degradation products. *Journal of pharmaceutical and biomedical analysis, 15*(12), 1867-1876.

Wani, A. A., Singh, P., Shah, M. A., Schweiggert-Weisz, U., Gul, K., & Wani, I. A. (2012). Rice starch diversity: Effects on structural, morphological, thermal, and physicochemical properties—A review. *Comprehensive reviews in food science and food safety, 11*(5), 417-436.

Wilken, R., Veena, M. S., Wang, M. B., & Srivatsan, E. S. (2011). Curcumin: A

review of anti-cancer properties and therapeutic activity in head and neck squamous cell carcinoma. *Molecular cancer, 10*(1), 12.

Xiao, C. (2013). Current advances of chemical and physical starch-based hydrogels. *Starch-Stärke, 65*(1-2), 82-88.

Xiao, C., & Yang, M. (2006). Controlled preparation of physical cross-linked starch-g-PVA hydrogel. *Carbohydrate Polymers, 64*(1), 37-40.

Xie, F., Yu, L., Su, B., Liu, P., Wang, J., Liu, H., & Chen, L. (2009). Rheological properties of starches with different amylose/amylopectin ratios. *Journal of Cereal Science, 49*(3), 371-377.

Yang, T., Tan, X., Huang, S., Pan, X., Shi, Q., Zeng, Y., . . . Zeng, Y. (2020). Effects of experimental warming on physicochemical properties of indica rice starch in a double rice cropping system. *Food Chemistry, 310*, 125981.

Yoo, D., & Yoo, B. (2005). Rheology of rice starch-sucrose composites. *Starch-Stärke, 57*(6), 254-261.

Yousefi, A., & Razavi, S. M. (2015). Dynamic rheological properties of wheat starch gels as affected by chemical modification and concentration. *Starch-Stärke, 67*(7-8), 567-576.

Yu, H., & Huang, Q. (2011). Investigation of the absorption mechanism of solubilized curcumin using Caco-2 cell monolayers. *Journal of agricultural and food chemistry, 59*(17), 9120-9126.

Zaidel, D. A., Chin, N., & Yusof, Y. (2010). A review on rheological properties and measurements of dough and gluten. *Journal of Applied Sciences(Faisalabad), 10*(20), 2478-2490.

Zhang, R., Zhang, Z., Zhang, H., Decker, E. A., & McClements, D. J. (2015). Influence of emulsifier type on gastrointestinal fate of oil-in-water

emulsions containing anionic dietary fiber (pectin). *Food Hydrocolloids, 45*, 175-185.

Zhang, Z., Wang, X., Yu, J., Chen, S., Ge, H., & Jiang, L. (2017). Freeze-thaw stability of oil-in-water emulsions stabilized by soy protein isolate-dextran conjugates. *LWT, 78*, 241-249.

Zhang, Z., Zhang, R., Zou, L., Chen, L., Ahmed, Y., Al Bishri, W., . . . McClements, D. J. (2016). Encapsulation of curcumin in polysaccharide-based hydrogel beads: Impact of bead type on lipid digestion and curcumin bioaccessibility. *Food Hydrocolloids, 58*, 160-170.

Zheng, B., Zhang, Z., Chen, F., Luo, X., & McClements, D. J. (2017). Impact of delivery system type on curcumin stability: Comparison of curcumin degradation in aqueous solutions, emulsions, and hydrogel beads. *Food Hydrocolloids, 71*, 187-197.

Zobel, H. (1988). Molecules to granules: a comprehensive starch review. *Starch-Stärke, 40*(2), 44-50.

Zobel, H., Young, S., & Rocca, L. (1988). Starch gelatinization: An X-ray diffraction study. *Cereal Chem, 65*(6), 443-446.

Zou, L., Zheng, B., Zhang, R., Zhang, Z., Liu, W., Liu, C., . . . McClements, D. J. (2016). Influence of lipid phase composition of excipient emulsions on curcumin solubility, stability, and bioaccessibility. *Food Biophysics, 11*(3), 213-225.

## 국문초록

# 4αGTase 처리 쌀 전분을 이용한 커큐민 포접 필드하이드로젤의 안정성에 관한 연구

커큐민 (Curcumin)은 *curcuma longa*의 뿌리에서 유래하는 천연 폴리페놀 화합물로 항암, 항염 및 항산화 효과 등의 생리활성을 지니고 있어 식품, 제약 등 여러 분야에서 널리 쓰이고 있다. 하지만 물에 대한 용해도가 매우 낮고 (약 11ng/ml), 자외선 및 온도 등의 외부 환경에 의해 쉽게 분해되기 때문에 낮은 생체이용률을 가진다. 그러므로 식품산업에서 커큐민을 활용함에 있어 제약이 된다.

이러한 커큐민의 낮은 용해도와 화학적 불안정성을 개선시키기 위해 나노에멀젼, 나노젤 등의 시스템을 통해 커큐민을 캡슐화하는 연구들이 진행되어왔다. 특히 수상층 내에 유화제로 둘러싸인 유상층으로 구성된 이중층의 에멀젼 시스템은 커큐민이 특정한 외부 자극에 따라 적절한 시점에서 방출될 수 있도록 하여 생체이용률을 향상시키기 위한 방안으로 널리 연구되었다. 그러나, 이러한 O/W 에멀젼은 열에 매우 불안정하며, 특정 환경에 노출되었을 때 시간에 따라 분해되기 쉬운 단점을 지닌다. 그러므로 최근에는 O/W 에멀젼의 점도를 높이고 젤네트워크를 형성하여 에멀젼의 안정성을 향상시키기 위하여 다당류를 에멀젼

의 수상층에 첨가하는 연구들이 진행되고 있다. 이러한 형태의 에멀젼을 $O/W_1/W_2$ 에멀젼이라고 하며 수상층에 분산된 하이드로젤 입자들이 지방구를 둘러싸고 있는 형태를 일컫는다. 따라서 무독성, 생체적합성을 지닌 다당류 기반 하이드로젤은 3차원 네트워크 구조를 형성하여 생리활성화합물의 운반체 역할로 활용될 수 있다. 수상층에 첨가될 수 있는 다당류의 한 종류로 쌀 전분을 들 수 있는데, 이 쌀 전분에 *Thermus Aquaticus* 4-a-glucanotransferase (4aGTase) 처리를 하여 변화된 물리화학적 특성을 지닌 효소처리 전분 기반 필드하이드로젤에 관한 연구가 아직 진행되지 않았다. 따라서, 본 연구는 4aGTase 처리 쌀 전분을 커큐민이 포접된 에멀젼의 수상층에 첨가하여 커큐민의 안정성과 생체이용률 향상을 증대시키는 것을 목적으로 한다. 쌀 전분이 첨가되지 않은 에멀젼과 비효소처리 쌀 전분 기반 하이드로젤을 비교군으로 정하였다.

먼저, 4aGTase 처리 전분의 다양한 물리화학적 특성을 분석하였다. 쌀 전분을 1시간, 24시간 및 96시간 동안 각각 처리한 후에 평균 분자량 분포 (HPSEC), 사슬 길이 분포 (HPAEC), Rheological properties, 점도 특성, Granular morphology (SEM), Starch crystallinity (XRD), 그리고 Iodine absorption capacity을 분석하였다. 평균 분자량 분포는 효소처리시간이 길어질수록 그 값이 작아졌으며 96시간 처리 시엔 fraction Ⅱ에서 가장 높은 분자량의 피크가

2.12× $10^5$ g/mol 에서 2.28 × $10^4$ g/mol로 이동하였고 fraction I 은 대체로 감소하였다. 이는 4aGTase의 dispropornation reaction 작용에 기인한 것으로 생각된다. 사슬 길이 분포는 효소 처리 시간이 길어짐에 따라 $B_2$와 $B_3$ 사슬의 비율이 높아졌다. 또한 steady-state flow 방법에 따른 점도 특성에서 효소처리 전분은 비효소처리전분에 비해 효소 처리 시간에 따라 점도가 현저하게 낮았으며, 효소처리전분 모두 V 타입의 XRD peak를 나타냈다. 커큐민이 포접된 에멀젼에 전분을 첨가하여 제조한 필드하이드로젤의 젤 특성을 분석하기 위하여 TPA를 측정해본 결과, 효소처리쌀전분 기반 필드하이드젤의 hardness는 비 효소처리쌀전분 기반 필드하이드젤보다 낮았으며 효소처리시간과 비례하여 감소하였다.

효소처리 쌀 전분 기반 필드하이드로젤의 커큐민 보호효과를 검증하기 위하여 열, UV 안정성을 측정하였으며 *in vitro* 소화시스템을 활용하여 소화과정을 거친 후의 커큐민 보유량과 생체이용률을 확인했다. 열 안정성에서는 24시간 가열 후 전분이 첨가되지 않은 에멀젼이 17.72% 로 가장 높은 열 안정성을 나타냈다. 가열 시작 후 3시간까지의 열 안정성 추이를 비교하면, 비효소처리 쌀 전분 기반 필드하이드로젤의 열 안정성은 처음 10분 이내에 급격히 감소했고 30분 후에 약 5.68% 정도의 잔류량을 가졌다. 이에 반해 효소처리쌀전분 기반 필드하이드

로젤은 가열 30분 후에 약 17.27%의 잔류량을 보였는데, 이는 앞선 비효소처리 쌀 전분 기반 필드하이드로젤보다 3.04배 높은 커큐민 열 안정성을 보였다. 필드하이드로젤의 UV안정성은 에멀젼 대비 최대 2.28배 향상되었다. 마지막으로 효소처리쌀전분 기반 필드하이드로젤의 *in vitro* 소화시스템을 거친 후의 커큐민 잔존량은 각각 80.2%, 85.0%, 그리고 90.1%로 커큐민 (34.7%), 에멀젼 (50.1%) 보다 유의적으로 높았다. 지방소화율의 경우 샘플 간의 유의미한 결과 차이는 나타나지 않았다. Confocal microscopy로 각 소화 단계 별 샘플 내의 지방구의 분포를 관찰해본 결과, 입 단계에서 에멀젼은 크기가 큰 coalescence가 나타났으나, 필드하이드로젤의 경우에는 flocculation만 나타났다. 위 단계에서도 에멀젼은 입 단계에서와 동일한 coalescence를 보였으며, 비효소처리 쌀 전분 기반 필드하이드로젤의 경우 flocculation과 지방구의 크기가 커진 coalescence가 나타났다. 효소처리쌀전분 기반 필드하이드로젤은 작은 크기의 coalescence가 나타난 것으로 보아 효소처리전분이 비효소처리전분보다 분자량이 작아 지방구 주위를 좀 더 촘촘하게 둘러싸 지방 분해와 관련된 효소 작용을 더디게 하여 에멀젼의 안정성을 높인 것으로 생각된다. 생체이용률 실험은 실험에 사용되는 샘플이 상당량 희석되어 사용되는데, 이로 인해 샘플 내의 상당히 낮은 농도의 커큐민이 함유되어 있어 정확한 측정이 어려운 것으로 나타났다.

따라서 이러한 결과로 미루어 보아 필드하이드로젤 시스템은 열 안정성에서 커큐민 보호효과가 나타나지 않으나 UV안정성과 *in vitro* 소화시스템과정에서는 향상된 커큐민 보호효과를 보였다. 특히 96GS로 만든 효소처리 쌀 전분 필드하이드로젤의 경우 *in vitro* 소화시스템과정에서 유의하게 높은 보호 효과가 나타났다. 따라서, 커큐민의 화학적 안정성 향상을 위한 생리활성물질전달시스템으로서 효소처리 쌀 전분 기반 필드하이드로젤의 적용가능성이 확인되었다.

**주요어: 효소변형전분, 커큐민, 필드하이드로젤, 안정성, 지방소화율, 생체이용률**

**학번: 2018-23057**